

NASA MEMO 4-23-59L

NASA MEMO 4-23-59L

**NASA**

**MEMORANDUM**

ANALYTICAL INVESTIGATION OF A FLICKER-TYPE ROLL CONTROL  
FOR A MACH NUMBER 6 MISSILE WITH AERODYNAMIC CONTROLS  
OVER AN ALTITUDE RANGE OF 82,000 TO 282,000 FEET

By Reginald R. Lundstrom and Ruth I. Whitman

Langley Research Center  
Langley Field, Va.

**NATIONAL AERONAUTICS AND  
SPACE ADMINISTRATION**

WASHINGTON

May 1959



NATIONAL AERONAUTICS AND SPACE ADMINISTRATION

---

MEMORANDUM 4-23-59L

---

ANALYTICAL INVESTIGATION OF A FLICKER-TYPE ROLL CONTROL  
FOR A MACH NUMBER 6 MISSILE WITH AERODYNAMIC CONTROLS  
OVER AN ALTITUDE RANGE OF 82,000 TO 282,000 FEET

By Reginald R. Lundstrom and Ruth I. Whitman

SUMMARY

An analytical investigation has been carried out to determine the responses of a flicker-type roll control incorporated in a missile which traverses a range of Mach number of 6.3 at an altitude of 82,000 feet to 5.26 at an altitude of 282,000 feet. The missile has  $80^\circ$  delta wings in a cruciform arrangement with aerodynamic controls attached to the fuselage near the wing trailing edge and indexed  $45^\circ$  to the wings. Most of the investigation was carried out on an analog computer.

Results showed that roll stabilization that may be adequate for many cases can be obtained over the altitude range considered, providing that the rate factor can be changed with altitude. The response would be improved if the control deflection were made larger at the higher altitudes. Lag times less than 0.04 second improve the response appreciably. Asymmetries that produce steady rolling moments can be very detrimental to the response in some cases. The wing damping made a negligible contribution to the response.

INTRODUCTION

There is current interest in roll-control systems for many hypersonic missiles, such as hypersonic gliders and missiles for defense against intercontinental ballistic missiles (ICBM), that employ a command guidance system. In many cases the roll orientation must be known so that the desired pitch or yaw can be applied from a ground station. The restoring moment for such a roll control may be aerodynamic or it may be a reaction moment. If the desired stabilization can be obtained using aerodynamic moments it would be expected that a large saving in weight may result since it would then be unnecessary to carry fuel for the reaction system.

It is well known that aerodynamic controls are very satisfactory at low altitudes and it is obvious that they are useless in free space. At what altitude aerodynamic controls become inadequate depends on the mass characteristics of the missile, the size, shape, and location of the control surfaces, and the maneuvers to be accomplished. For roll stabilization it is probably sufficient merely to hold the missile at a certain known roll orientation and overcome any rolling moments due to asymmetries in construction and due to combined pitching and yawing motions. Since the roll coupling moments and moments due to asymmetry are a function of the dynamic pressure just as is the available moment from ailerons, there would appear to be good promise for aerodynamic roll stabilization over a wide altitude range. The response characteristics, however, would be expected to differ profoundly with altitude. A missile would probably handle like a small model airplane at low altitudes and like a large battleship at very high altitudes.

Much work has been done on roll-control systems of various types (see, e.g., refs. 1 to 3) but none of this work covers the effects of a large range of altitude or rapid changes in altitude. The analytical investigation reported herein covers the roll-response characteristics of a missile from a Mach number of 6.3 at 82,000 feet to a Mach number of 5.2 at 282,000 feet with a corresponding dynamic pressure range from 1,500 to 0.15 lb/sq ft. Of the possible roll-control systems, both the proportional displacement-plus-rate control and the flicker displacement-plus-rate control appeared promising provided that the rate factor could be changed with changing altitude. Since, at the present time, simplicity of missile components appears to be such a creditable objective, the flicker system was chosen for this investigation because it is generally the simpler of the two systems. This report shows some effects of rate factor, magnitude of control moment, system time lag, magnitude of disturbance, construction asymmetry, and aerodynamic damping on the missile roll response. Some responses are also determined during rapid changes in altitude.

#### SYMBOLS

A	half amplitude of steady-state hunting oscillation, deg
b	wing span, 2.05 ft
$C_l$	rolling-moment coefficient, $\frac{\text{Rolling moment}}{qSb}$
$C_{l_p}$	roll damping coefficient of all four wing panels, $\frac{\partial C_l}{\partial \frac{pb}{2V}}$ per radian

$C_{l\delta}$	control effectiveness coefficient, $\frac{\partial C_l}{\partial \delta}$ per degree
$E = \phi_1 - \phi_0$	(see fig. 14(a))
$F_1, F_2, F_3, F_4$	block-diagram designations (see fig. 14(a))
$h$	altitude of missile, ft
$I_x$	moment of inertia about longitudinal axis, slug-ft <sup>2</sup>
$j = \sqrt{-1}$	
$L_0$	rolling moment due to an asymmetry in model, ft-lb
$L_p$	roll damping derivative, $C_{l_p} \frac{b^2}{2V} qS$ , ft-lb/radian/sec
$L_\delta$	control effectiveness derivative, foot pounds per degree aileron deflection, $C_{l_\delta} qSb$
$M$	Mach number
$n$	block-diagram designation of output from signal-reversal relay (see fig. 14(b))
$p$	roll angular velocity, radians/sec
$q$	dynamic pressure, $\frac{1}{2}\rho V^2$ , lb/sq ft
$S$	exposed wing area per plane, 3.06 sq ft
$s$	Laplace transform operator
$t$	time from launching, sec
$t_1$	time to reach steady-state hunting oscillation, sec
$t_2$	time to reach 2° amplitude, sec
$V$	velocity, ft/sec
$\delta$	aileron deflection ( $\delta = 1^\circ$ means one aileron up $1^\circ$ and the other aileron down $1^\circ$ ), deg

$\epsilon$	block-diagram designation for error signal (fig. 14)
$\Lambda$	rate factor (differentiator output per unit roll velocity), radians/radian/sec or sec
$\rho$	air density, slugs/cu ft
$\tau$	time between signal to reverse controls and actual reversal of controls, sec
$\phi$	bank angle, radians unless otherwise stated
$\dot{\phi}$	roll rate (same as symbol $p$ ), radians/sec
$\ddot{\phi}$	roll acceleration, radians/sec <sup>2</sup>
$\phi_i$	initial bank angle, deg
$\phi_1$	roll input signal (fig. 14)
$\phi_o$	roll output signal (fig. 14)
$\dot{\phi}_o$	roll velocity output signal (fig. 14)
$\omega$	natural frequency of hunting oscillations, radians/sec

#### MISSILE AND TRAJECTORY

The research missile considered in this investigation was a cruciform delta-wing configuration having 80° sweepback of the wing leading edges. The control surfaces were located near the wing trailing edges and were indexed 45° to the wings. A sketch of the model, together with pertinent dimensional and mass characteristics, is shown in figure 1. Estimates of the aileron effectiveness parameter  $C_{l\delta}$  and the damping-in-roll derivative  $C_{lp}$  used in the analysis are shown in figure 2.

The missile was calculated to have acquired its velocity and altitude 59 seconds after take-off by means of a four-stage boost arrangement made up of rockets in current use. This particular trajectory was selected because it covered the desired altitude range at a rate of climb of the order considered for an anti-ICBM missile. The velocity, altitude, and Mach number calculated for this arrangement during the coasting flight are presented as a function of time in figure 3 and the dynamic pressure is presented in figure 4.

## ROLL-CONTROL SYSTEM

The roll-control system considered in this investigation was physically very similar to that described in reference 2. A block diagram of the system is presented in figure 5. The detection of an error caused the servo to deflect the ailerons against a stop producing an aerodynamic rolling moment to eliminate the error. A feedback loop, the output of which was proportional to the rolling velocity, was in parallel with the feedback loop containing the output from the roll angular displacement. The error signal was the difference between the desired output (represented by a roll displacement of zero, and a roll velocity of zero) and the sum of the actual outputs from the displacement- and rate-feedback loops. As the error signal changed sign the ailerons were driven from one set of stops to the other. Throughout this report, except where otherwise noted, the stops were considered to be at  $5^\circ$  aileron and  $-5^\circ$  aileron. In this report it was assumed that the rate factor could be changed at will; however, an effort was made to keep this variation to a minimum. In a flicker system, a lag time always exists between the time the error signal changes sign and the time the control moment changes sign. Throughout this report, except where otherwise noted, this time lag was taken to be 0.04 second and was not a function of the amount of control deflection.

### Method of Analysis

The response of the airframe about its longitudinal axis may be expressed by the following single-degree-of-freedom equation:

$$L_\delta \delta + L_0 = I_x \ddot{\phi} - L_p \dot{\phi}$$

The control moment  $L_\delta \delta$  changed sign  $\tau$  seconds after  $\phi + \Lambda \dot{\phi} = 0$ . The following methods were considered for determining the response of the roll-control—airframe combination:

- (1) Calculation of steady-state hunting frequency and amplitude using the method of reference 2
- (2) Use of servomechanism phase-angle plots (see appendix)
- (3) Analog simulation
- (4) Graphical solution of response (ref. 1)

Method (1) was not used in this particular case because the values of  $L_\delta \delta$ ,  $L_p$ , and  $I_x$  for the example missile made the equations very insensitive. Method (2), which gives only the amplitude and frequency of the

steady-state hunting oscillation, was very useful, particularly as a rapid method of determining the proper range of  $\Lambda$  to be investigated by other methods. Method (3) was used for most of the data presented in this report and is discussed in more detail in a succeeding section. Method (4) is a very lengthy step-by-step method of solution but was used to good advantage at times to check results obtained from the analog computer.

### Analog Simulation

The computer used for this investigation gave an electrical analog of the rolling motion of the airframe—roll-control combination, under its flight conditions, when the airframe was displaced a known amount from its reference position and released. The single-degree-of-freedom equation for moments about the missile longitudinal-body axis was used along with networks and relays to obtain a time lag  $\tau$  and to reverse the signal when  $(\phi + \Lambda\dot{\phi})$  changed sign. In all analog runs machine time was made equal to real time. The disturbance corresponded to holding the missile at an initial bank-angle error of  $10^\circ$  (roll velocity equal to zero) and releasing it, except for specific runs when the effect of the magnitude of the disturbance was investigated. During runs to investigate the effect on the response of various individual parameters, such as, rate factor, time lag, control deflection, and so forth, the dynamic pressure was held constant at a value corresponding to the flight time listed. However, since the rapidly varying dynamic pressure could materially affect the response characteristics, final runs were made using an electromechanical device to give the proper simulated variation of dynamic pressure with time. Roll disturbances were introduced at predetermined intervals and the responses were recorded. The rate factor  $\Lambda$  was varied in steps and was always held constant over each individual response. In response curves shown (e.g., fig. 6) the amplitudes of the traces labeled  $L_6\delta$  are not indicative of the actual values of  $L_6\delta$  used for different responses. Since over the range of the investigation  $L_6\delta$  varied by about  $10^4$ , changes in sensitivity of the recorder were made between runs so that control reversal could be more readily observed. An outline showing the range of test variables investigated at the various flight conditions is presented in table I.

### RESULTS AND DISCUSSION

The requirements of a roll-stabilization system are strictly dependent upon the size of the roll disturbances the missile is expected to encounter. The largest disturbances in the example missile would occur when the missile separates from its previous stage, which in this case occurs at the lowest altitude considered. All disturbances after this



separation would probably be aerodynamic. An example where this is not the case would be a missile having reaction controls in pitch and yaw that produce a rolling moment due to thrust misalignments. The ability of the control system to damp the resulting airframe rolling motion in an acceptable manner is influenced by the rate factor  $\Lambda$ , the control moment  $L_\delta \delta$ , the system time lag  $\tau$ , and the aerodynamic damping of the airframe  $L_p$ . Quantities regarded as important in assessing the adequacy of the roll-control system are (1) the frequency and amplitude of the steady-state hunting oscillation, (2) the time to reach the steady-state hunting frequency following a disturbance, and (3) the time to reach a roll displacement of less than  $2^\circ$ . These factors are listed for all cases in table II.

### Effects of Rate Factor

Since any system involving a changing rate factor becomes more complex as the range of variation becomes greater, an effort was made to hold the rate-factor variation to a minimum. This was accomplished by making the transient about deadbeat when stabilization started at 82,000 feet and by using the lowest reasonable value of damping at the highest altitude condition, 282,000 feet. Responses obtained for various rate factors at various altitude conditions are shown in figure 6. Listings of the steady-state hunting frequency, the time to reach steady-state hunting frequency, and the time to reach a roll displacement of less than  $2^\circ$  are presented in table II(a) for varying rate factors. Values of  $\phi_i = 10^\circ$ ,  $\tau = 0.04$  second, and  $\delta = 5^\circ$  were used in all these cases.

From the summation of the calculated phase angles shown in figure 7, it was found that there was little variation in steady-state hunting frequency  $\omega$  over the entire altitude range. The expression for the amplitude of the steady-state hunting oscillation  $A$  given in the appendix may be reduced to

$$A = \pm \frac{4L_\delta \delta}{\pi \omega} \frac{57.3}{\sqrt{L_p^2 + I_x^2 \omega^2}}$$

Since  $L_p^2$  is negligible compared with  $I_x^2 \omega^2$  (discussed further in the section entitled "Effects of Wing Damping"), the value of  $A$  is approximately proportional to  $L_\delta \delta$  or  $q$ . Hence, the larger amplitudes should occur at the low altitudes. Analog results in figure 6 or table II(a) confirm these trends.

The steady-state hunting frequencies obtained from the analog (table II(a)) are much lower than the steady-state hunting frequencies obtained from the phase plots (fig. 7). It is believed that the system used to produce the desired time lags for the analog results did not give a very good approximation for a square wave. This is indicated by the shape of the  $I_{\delta}\delta$  traces in figures 6(c) and 6(d). If a value of  $\tau = 0.05$  second had been used in figure 7 instead of  $\tau = 0.04$  second, the hunting frequency would have been in good agreement with the analog results. Figure 6 shows that the time to reach the steady-state hunting frequency becomes very large at the higher altitudes. This may not be quite so serious as it at first appears, since in actual flight it would be expected that  $\phi_1$ , representing the magnitude of the disturbance, would be likely to be much smaller at the high altitudes than at the low altitudes. It may be noted that, although values of the rate factor  $\Lambda$  may be chosen that improve the response, the system is not overly sensitive in this respect at a given altitude, and great precision in adjusting the rate factor is not required.

#### Effect of Control Moment

The effect of increasing the aileron deflection  $\delta$  to obtain a larger corrective moment from the ailerons is shown in figure 8 for flight times of 59, 80, and 170 seconds. It may be noted that  $\delta = 20^\circ$  produced a steady-state hunting amplitude that may be objectionably large at the low altitudes but was well within the  $\pm 2^\circ$  tolerance at the high altitudes. At the high altitudes the time to damp to the steady-state hunting oscillations was considerably shortened, as expected, for the larger values of  $\delta$  as shown in table II(b). This table shows that if the additional complication could be tolerated the roll response could be appreciably improved by incorporating a device which increases the value of  $\delta$  at the high altitudes.

#### Effect of Magnitude of Disturbance

Since it would be expected that in many cases the roll disturbances might be smaller at the high altitudes, runs were made at 59 seconds, ( $\Lambda = 0.2$ ), 80 seconds ( $\Lambda = 0.2$ ), and 170 seconds ( $\Lambda = 3.5$ ) at three values of  $\phi_1$ . These results are shown in figure 9 and in table II(c). At the low altitude the times to damp to the steady-state hunting frequency for  $\phi_1 = 5^\circ, 10^\circ, \text{ and } 20^\circ$  were all very short. As would be expected for  $t = 80$  seconds and  $t = 170$  seconds the time to reach the steady-state hunting frequency was approximately proportional to the size of the initial disturbance.

### Effect of Asymmetry

Construction tolerances for a missile means that the roll equation will have a term  $L_0$ , which is the rolling moment caused by wing or control-surface misalignments. The effect of such an asymmetry and its direction is shown in figure 10 at flight times of 70 and 80 seconds. The asymmetric rolling moment  $L_0$  during these runs was made as large as the rolling moment resulting from  $2.5^\circ$  of aileron deflection. It is very apparent that when the disturbance ( $\phi_1 = 10^\circ$ ) had a sign opposite to that of  $L_0$  there is a large overshoot and the time to reach the steady-state hunting frequency is much longer than if no asymmetry existed. This is to be expected since the asymmetry acts as if the control-surface stops were set at  $2.5^\circ$  and  $-7.5^\circ$  instead of at  $5^\circ$  and  $-5^\circ$ . The equivalent of  $7.5^\circ$  of aileron deflection applied corrective rolling moment to overcome the initial error in bank angle, but the equivalent of only  $2.5^\circ$  of aileron was available to prevent the overshoot. This caused the initial correction to be more rapid and the overshoot large. On the other hand if the disturbance had the same sign as  $L_0$ , the time to reach steady-state hunting frequency was less than if no asymmetry existed. In this case the initial correction was slower, since it resulted from the equivalent of only  $2.5^\circ$  of aileron, and the equivalent of  $7.5^\circ$  of aileron opposed the overshoot causing the final correction to be almost deadbeat.

Responses run at 60 seconds indicated the tendency to overshoot to be much less (table II(d)). Limitations of the computer precluded making runs at higher altitudes. Comparison of the responses in figure 10 might lead to the belief that the effects of asymmetry are aggravated by higher altitudes. Here, again, it must be remembered that the disturbances might be proportionally smaller at the higher altitudes. However, it is apparent that the effects of a very large asymmetry could seriously affect the response of a flicker-type roll-control system and should be watched closely.

### Effect of Lag Time

Lag times are seldom accurately known until the roll-control system is actually built and tested. The value of 0.04 second used for most tests was considered to be a reasonable value for electromagnetic actuators of the type considered for the research missile. From the phase angles plotted in figures 7(a) and 7(b) the lag time is the most critical factor in determining the steady-state hunting frequency because of the steep slope of curve A at the steady-state hunting frequency. From the relationship established in the section "Effects of Rate Factor" that the amplitude of the steady-state hunting oscillation for the example missile is approximately inversely proportional to the hunting frequency,

the lag time is also the most critical factor affecting this amplitude. Analog responses made at  $t = 59$  seconds,  $h = 82,000$  feet, and  $V = 6,100$  ft/sec for lag times of 0.02, 0.03, 0.04, and 0.05 second which are presented in figure 11 clearly show this sensitivity. Shortening the lag time from 0.05 to 0.02 second reduces the amplitude of the steady-state hunting oscillation from  $1.5^\circ$  to  $0.3^\circ$  as indicated in table II(e). Thus, the great advantage of a shorter lag time when variations in altitude are considered is that  $L_3\delta$  may be increased to improve the response at high altitudes and still keep the oscillation amplitude within tolerance at the low altitude. Values listed in table II(e) for lag times of 0.02, 0.04, and 0.05 at 170 seconds show that the time to reach the steady-state hunting frequency is about 17 percent less for  $\tau = 0.02$  second than for  $\tau = 0.05$  second.

#### Effect of Wing Damping

Since such large values of rate factor  $A$  were required and the values of  $C_{l_p}$  were small, it was suspected that the wing damping was producing very little effect on the roll response. This effect is apparent from the equation for the amplitude of the steady-state hunting oscillation

$$A = \pm \frac{4I_G\delta}{\pi\omega} \frac{57.3}{\sqrt{I_p^2 + I_x^2\omega^2}}$$

where  $I_x\omega$  has a value of about 20, and  $I_p$  varies from 0.288 at the low altitude to 0.000038 at the high altitude. Thus, the value of  $I_p^2$  is insignificant compared with the value of  $I_x^2\omega^2$ . Figure 12 shows responses run at  $t = 70$  seconds for  $L_p$  equal to zero and  $L_p$  equal to its normal value of 0.074. These responses appear identical. Responses run at other flight times also appeared to be the same (table II(f)). This identicalness means that in the case of the example missile, except for the effect on  $I_x$ , it makes no difference to the roll-control system whether the missile has wings or not.

#### Effects of Rapidly Changing Altitude

In all responses presented previously it has been assumed that the missile remained at a constant altitude from the time the disturbance

originated through the time the steady-state hunting frequency was reached. In actual flight the missile would have covered a substantial change in altitude over this period. By assuming that  $L_p = 0$  it was possible to make analog responses varying  $L_{\delta}$  in the same manner as it would vary if the missile followed the flight path shown in figure 3. Each of these responses, presented in figure 13, is initiated at a different altitude and covers the altitude and velocity range indicated in the figure. The values of  $\Lambda$  used are shown in the figure and were held constant for each individual run. It may be seen that while the responses differ from the constant-altitude responses, no instabilities were present.

### CONCLUSIONS

An analytical investigation of a flicker-type roll control installed in a research missile having  $80^\circ$  delta wings and capable of reaching a Mach number of 6 which traveled through an altitude range of 82,000 feet to 282,000 feet indicated the following conclusions:

1. Stabilization that is adequate for many cases was obtained provided that the rate factor could be changed by a factor of 10 or 20 over the altitude range. The larger rate factors are required at the higher altitudes in order to reduce the time to reach the steady-state hunting frequency.
2. Increasing the rolling moment from the ailerons improved the performance at the high altitudes but caused the amplitude of the hunting oscillations to be objectionably large at the low altitudes.
3. The time required to reach the steady-state hunting oscillations following a disturbance was approximately proportional to the size of the disturbance.
4. Asymmetries that cause a rolling moment had a detrimental effect on the response if the disturbance rolling moment was opposite to the rolling moment caused by the asymmetry. If they are in the same direction the response is improved.
5. Shortening the lag time from 0.05 to 0.02 second reduced the steady-state hunting amplitude at the low altitude by a factor of 5 and reduced the time to reach the steady-state hunting oscillation at the high altitude by about 17 percent.
6. The wing damping made a negligible contribution to the response.

7. The rapid change in altitude, between the time of the disturbance and the time the steady-state hunting frequency was reached, caused no instability of the system.

Langley Research Center,  
National Aeronautics and Space Administration,  
Langley Field, Va., February 5, 1959.

## APPENDIX

## ANALYSIS OF SERVOMECHANISM BLOCK DIAGRAM

The flicker-type roll-control system with rate-plus-position feedback is inherently a neutrally stable system. A neutrally stable system means that the phase angle of the output over the input is  $-180^\circ$  and that the steady-state oscillation has a constant amplitude.

Figure 14(a) is a block diagram of the flicker-type roll-control system. A basic assumption of this analysis was that the signal-reversal relay was perfect; therefore, there was no hysteresis or dead zone so that there was no phase-angle shift in the signal-reversal relay. (See ref. 4.) It was therefore possible to use the methods of block-diagram algebra as explained in standard servomechanism texts, for example, references 5 and 6, to derive the following equations:

$$\epsilon = \phi_1 - (\phi_0 + \Lambda \dot{\phi}_0) \quad (1)$$

$$\text{Relay} \left\{ \begin{array}{ll} n = +1 & \epsilon > 0 \\ n = -1 & \epsilon < 0 \end{array} \right\} \quad (2)$$

$$\frac{\phi_0}{\delta} = F_3 \quad (3)$$

$$\frac{\phi_0}{\epsilon} = F_1 F_2 F_3 \quad (4)$$

$$\frac{\phi_0}{E} = \frac{F_1 F_2 F_3}{1 + F_4 F_1 F_2 F_3} \quad (5)$$

$$\frac{\phi_0}{\phi_1} = \frac{F_1 F_2 F_3}{1 + F_4 F_1 F_2 F_3 + F_1 F_2 F_3} = \frac{F_2 F_3}{\frac{1}{F_1} + F_2 F_3 (1 + F_4)} \quad (6)$$

The denominator of the closed-loop equation (eq. (6)) set equal to zero is the characteristic equation of the system and is used to determine the stability of the system.

The equation applicable to the airframe is the single-degree-of-freedom roll-control equation

$$I_X \ddot{\phi} - L_p \dot{\phi} = \pm L_\delta \delta \quad (7)$$

Taking the Laplace transform

$$I_X s^2 \phi - L_p s \phi = \pm L_\delta \delta \quad (8)$$

the transfer function is

$$\frac{\phi}{\delta} = \frac{\frac{L_\delta}{-L_p}}{s \left( 1 + \frac{I_X}{-L_p} s \right)} \quad (9)$$

The Laplace transform of a time delay is  $e^{-\tau s}$  and of the differentiator is  $\Lambda s$ . In figure 14(b) the appropriate transfer functions have replaced the block designation of figure 14(a). Substituting the transfer functions for the block designations in the characteristics of equation (6) and realizing that  $F_1$  now designates the output fundamental of the signal-reversal relay gives

$$\frac{1}{F_1} = e^{-\tau s} \frac{\frac{L_\delta \delta}{-L_p}}{s \left( 1 + \frac{I_X}{-L_p} s \right)} (1 + \Lambda s) \quad (10)$$

Substituting  $j\omega$  for  $s$  in equation (11) gives

$$\frac{1}{F_1} = e^{-j\omega\tau} \frac{\frac{L_\delta \delta}{-L_p}}{j\omega \left( 1 + \frac{I_X}{-L_p} j\omega \right)} (1 + \Lambda j\omega) \quad (11)$$

It is possible to express a complex number as a magnitude with an associated phase angle. As previously stated the phase angle of this system is  $-180^\circ$ .

In order to find the value of  $\omega$  when the phase angle is  $-180^\circ$  it is possible to plot the phase angle associated with the various terms of equation (11) on semilogarithmic paper, as shown in figure 7, by



utilizing phase-angle templates and/or by calculating and plotting the phase angles (ref. 4). Phase angles are additive. Since the half amplitude (A) of the steady-state oscillation is directly related to the value of  $\omega$  when the phase angle is  $-180^\circ$  by the expression

$$A = \left| \frac{\frac{4}{\pi} \left( \frac{I_D \delta}{-I_p} \right) (57.3)}{j\omega \left( 1 + \frac{I_x}{-I_p} j\omega \right)} \right| = \frac{4 I_D \delta}{\pi \omega} \frac{57.3}{\sqrt{I_p^2 + I_x^2 \omega^2}}$$

it is possible to adjust the variable parameters  $\tau$  and  $\Lambda$  (within certain physical limitations) to obtain an acceptable steady-state error.

## REFERENCES

1. Pitkin, Marvin, and Seacord, Charles L.: Correlation of the Computed Rolling Motion of the MX-570 (Tiamat-Model B) Guided Missile With That Obtained in Flight. NACA MR L6C09, Army Air Forces, 1946.
2. Curfman, Howard J., Jr.: Theoretical Analysis of the Rolling Motions of Aircraft Using a Flicker-Type Automatic Roll Stabilization System Having a Displacement-Plus-Rate Response. NACA RM L8K23a, 1949.
3. Gardiner, Robert A., and Zarovsky, Jacob: Rocket-Powered Flight Test of a Roll-Stabilized Supersonic Missile Configuration. NACA RM L9K01a, 1950.
4. Kochenburger, Ralph J.: A Frequency Response Method for Analyzing and Synthesizing Contactor Servomechanisms. Trans. AIEE, vol. 69, pt. I, 1950, pp. 270-283.
5. Nixon, Floyd E.: Principles of Automatic Controls. Prentice-Hall, Inc., c.1953.
6. Brown, Gordon S., and Campbell, Donald P.: Principles of Servomechanisms. John Wiley & Sons, Inc., 1948.

TABLE I  
ANALOG TEST PROGRAM

Flight conditions				Test variables						
t, sec	h, ft	M	q, lb/sq ft	$\Delta$ , sec (fig. 6)	$\delta$ , deg (fig. 8)	$\phi_1$ , deg (fig. 9)	$L_0$ , ft-lb (fig. 10)	$\tau$ , sec (fig. 11)	$L_p$ , ft-lb/radian/sec (fig. 12)	
59	82,000	6.30	1,500	0.1 to 0.4	5 to 20	5 to 20	-----	0.02 to 0.05	0.288, 0	
60	89,000	6.19	1,000	-----	-----	-----	$\pm 2.5L_0$	-----	-----	
70	123,000	5.55	180	.1 to .4	-----	-----	$\pm 2.5L_0$	-----	.037, 0	
80	152,000	5.11	49.0	.2 to .4	5 to 20	5 to 20	$\pm 2.5L_0$	-----	.013, 0	
90	180,000	5.03	15.8	.4 to .6	-----	-----	-----	-----	-----	
100	204,000	5.16	5.80	.3 to .9	-----	-----	-----	-----	-----	
110	225,000	5.32	2.40	.7 to 1.3	-----	-----	-----	-----	-----	
120	243,000	5.46	1.10	.9 to 1.6	-----	-----	-----	-----	-----	
130	257,000	5.44	.56	1.2 to 2.5	-----	-----	-----	-----	-----	
140	268,000	5.36	.32	2.0 to 3.0	-----	-----	-----	-----	-----	
150	276,000	5.30	.21	2.4 to 3.2	-----	-----	-----	-----	-----	
170	282,000	5.26	.15	3.5	5 to 20	1 to 10	-----	.02 to .05	-----	

TABLE II  
ANALOG RESULTS  
(a) Effects of rate factor

t, sec	$\Delta$ , sec	$\omega$ , radians/sec	A, deg	$t_1$ , sec	$t_2$ , sec
59	0.1	22	2	0.2	----
59	.2	25	1	.2	----
59	.3	25	1	.2	----
59	.4	28	.3	.1	----
70	.1	22	.3	3.0	5.6
70	.2	25	.2	.9	.6
70	.3	25	---	.5	.4
70	.4	25	---	.4	.4
80	.2	25	---	4.8	3.4
80	.3	25	---	3.4	1.4
80	.4	25	---	2.2	1.4
90	.4	25	---	6.2	5.2
90	.5	25	---	4.6	2.5
90	.6	25	---	3.7	2.8
100	.5	25	---	10.8	8.0
100	.4	25	---	8.0	5.2
100	.5	28	---	6.0	4.8
100	.6	28	---	5.0	4.2
100	.7	25	---	4.0	3.0
100	.8	25	---	3.6	2.0
100	.9	25	---	3.0	2.2
110	.7	25	---	10.0	7.6
110	.8	28	---	9.0	7.2
110	.9	25	---	7.6	6.4
110	1.0	25	---	6.2	3.2
110	1.1	28	---	6.0	3.4
110	1.2	28	---	5.8	3.6
110	1.3	25	---	5.7	3.4
120	.9	22	---	17.0	11.6
120	1.0	25	---	14.4	11.0
120	1.1	25	---	13.2	10.6
120	1.2	25	---	12.4	9.6
120	1.3	25	---	11.6	9.6
120	1.4	25	---	10.4	5.0
120	1.5	25	---	10.0	5.0
120	1.6	25	---	9.0	5.2
130	1.2	31	---	24.8	16.8
130	1.3	31	---	22.6	16.0
130	1.5	31	---	19.6	15.4
130	1.7	31	---	17.6	14.3
130	1.9	28	---	15.4	13.2
130	2.2	28	---	13.0	7.0
130	2.5	28	---	11.6	7.2
140	2.0	31	---	26	20.8
140	2.2	28	---	22.8	19.0
140	2.4	25	---	20.8	20.2
140	2.6	25	---	18.8	9.0
140	2.8	25	---	17.0	9.4
140	3.0	28	---	16.2	9.4
150	2.4	31	---	32.4	24.8
150	2.6	28	---	29.6	24.0
150	2.8	25	---	27.2	23.0
150	3.0	25	---	25.0	21.2
150	3.2	25	---	22.2	11.6
170	3.5	25	---	29.0	24.8

TABLE II.- ANALOG RESULTS - Continued

## (b) Effects of control moment

t, sec	$\Lambda$ , sec	$\omega$ , radians/sec	A, deg	$t_1$ , sec	$t_2$ , sec	$\delta$ , deg
59	0.2	25	1.0	0.1	----	5
59	.2	25	1.5	.1	----	7.5
59	.2	25	2.0	.1	----	10
59	.2	25	3.5	.1	----	15
59	.2	25	4.0	.1	----	20
80	.2	31	---	4.6	3.6	5
80	.2	31	---	3.2	2.8	7.5
80	.2	31	---	2.6	2.0	10
80	.2	31	---	1.8	1.0	15
80	.2	31	.2	1.4	.8	20
170	3.5	25	---	29	24.8	5
170	3.5	25	---	21	12.6	7.5
170	3.5	28	---	16.2	11.0	10
170	3.5	31	---	8.8	8.2	15
170	3.5	31	---	7.0	7.4	20

## (c) Effect of disturbance magnitude

t, sec	$\Lambda$ , sec	$\omega$ , radians/sec	A, deg	$t_1$ , sec	$t_2$ , sec	$\phi_1$ , deg
59	0.2	25	1	0.2	----	5
59	.2	25	1	.2	0.10	10
59	.2	25	1	.2	.25	20
80	.2	25	-	1.4	.3	5
80	.2	25	-	2.5	1.7	10
80	.2	25	-	4.5	3.6	20
170	3.5	25	-	2.4	----	1
170	3.5	28	-	4.5	0	2
170	3.5	28	-	15.0	8.2	5
170	3.5	28	-	29.5	26.2	10

TABLE II.- ANALOG RESULTS - Concluded

(d) Effect of asymmetry ( $L_0 = \pm 2.5I_0\delta$ )

t, sec	$\Lambda$ , sec	$\omega$ , radians/sec	A, deg	$t_1$ , sec	$t_2$ , sec	Sign of $L_0$ as compared with that of $\phi_1$
60	0.2	22	1.5	0.3	0.3	Same
60	.2	19	1.5	.5	.4	Opposite
70	.2	19	---	.5	.5	Same
70	.2	19	---	1.5	1.5	Opposite
80	.2	16	---	2.0	1.2	Same
80	.2	19	---	5.3	3.8	Opposite

(e) Effect of lag time

t, sec	$\Lambda$ , sec	$\omega$ , radians/sec	A, deg	$t_1$ , sec	$t_2$ , sec	$\tau$ , sec
59	0.2	44	0.3	0.1	0.5	0.02
59	.2	31	.5	.1	.5	.03
59	.2	25	1.0	.1	.3	.04
59	.2	22	1.5	.1	.4	.05
170	3.5	28	---	25.8	13.2	.02
170	3.5	28	---	29	24.8	.04
170	3.5	28	---	31	26	.05

(f) Effect of wing damping

t, sec	$\Lambda$ , sec	$\omega$ , radians/sec	A, deg	$t_1$ , sec	$t_2$ , sec	$L_p$ , $\frac{\text{ft-lb}}{\text{radian/sec}}$
59	0.2	28	1	0.3	0.2	0.288
59	.2	28	1	.3	.2	0
70	.2	28	-	1.0	.5	.038
70	.2	28	-	1.0	.5	0
80	.2	28	-	5.0	3.6	.010
80	.2	28	-	5.0	3.6	0

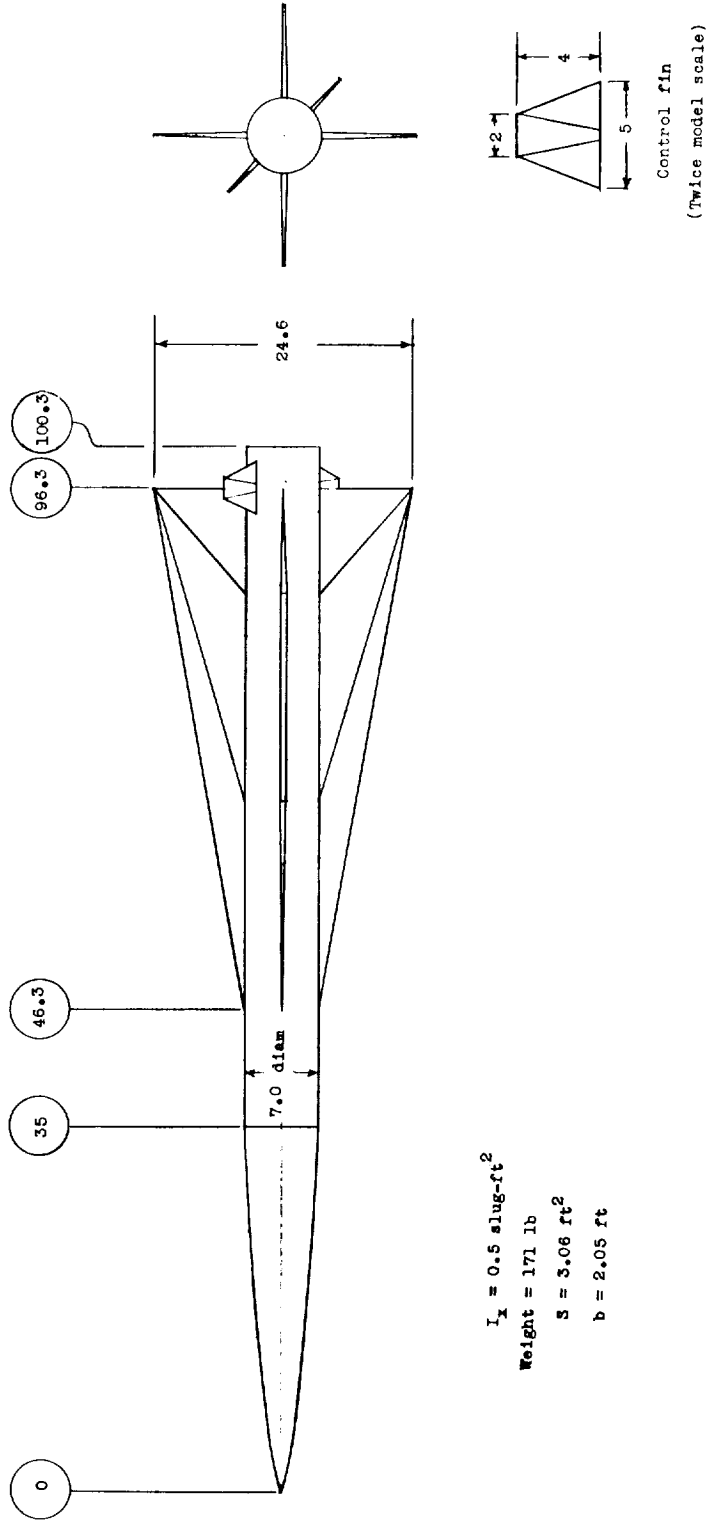


Figure 1.- General arrangement of model. All dimensions are in inches.

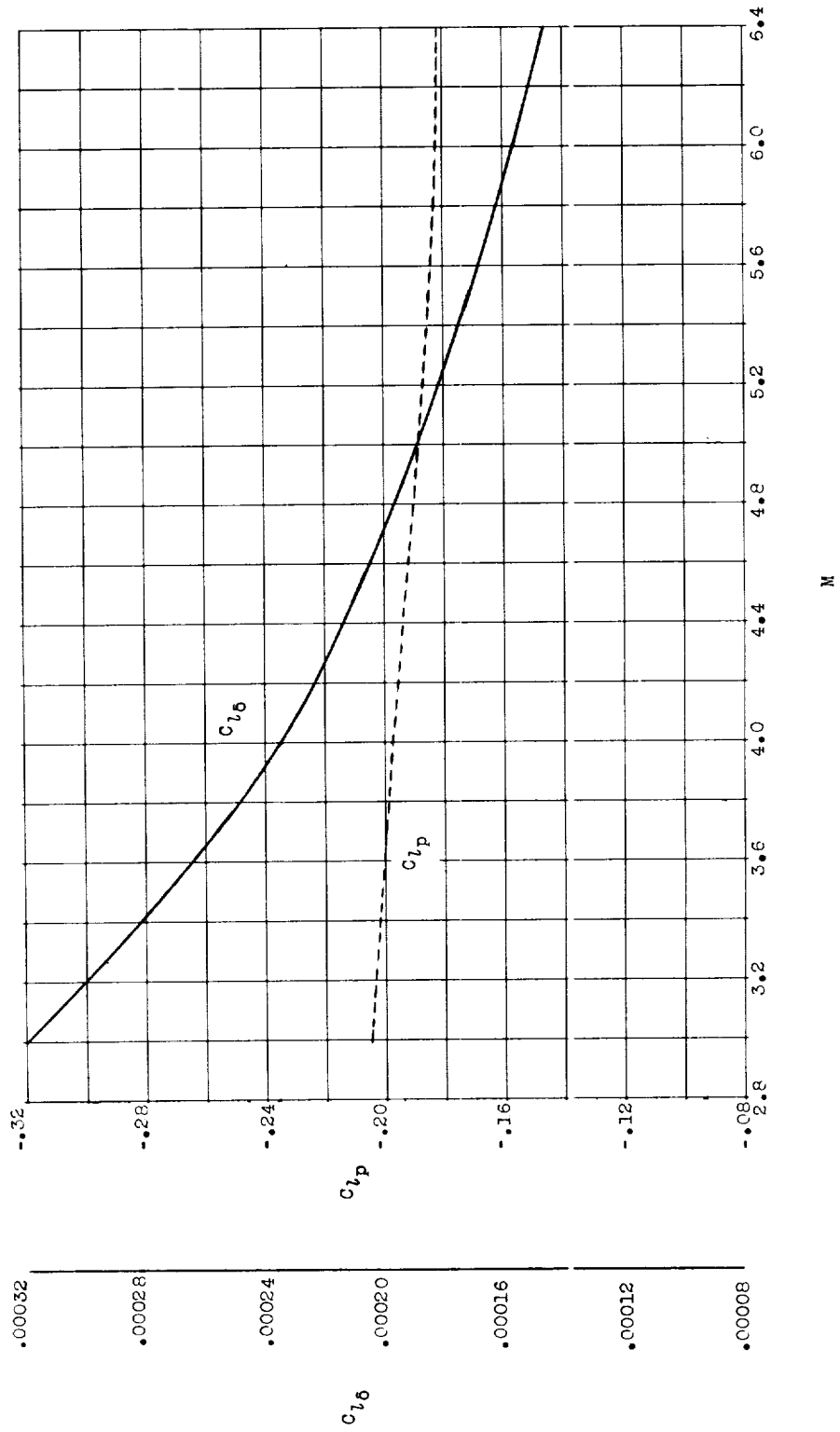


Figure 2.- Estimated values of  $C_{lp}$  and  $C_{l\delta}$  plotted against Mach number.



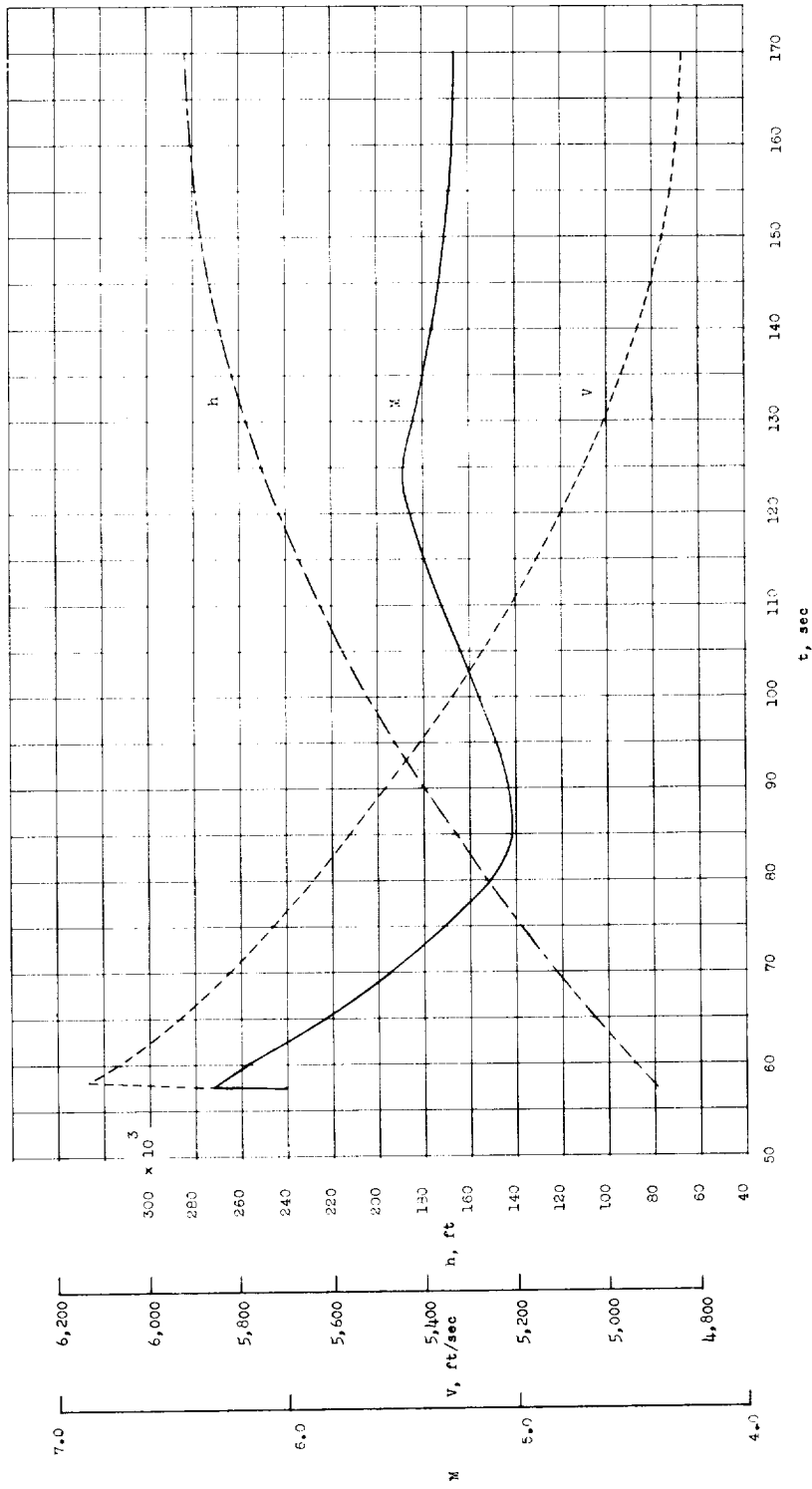


Figure 3.- Calculated values of Mach number, velocity, and altitude during coasting flight as a function of flight time.

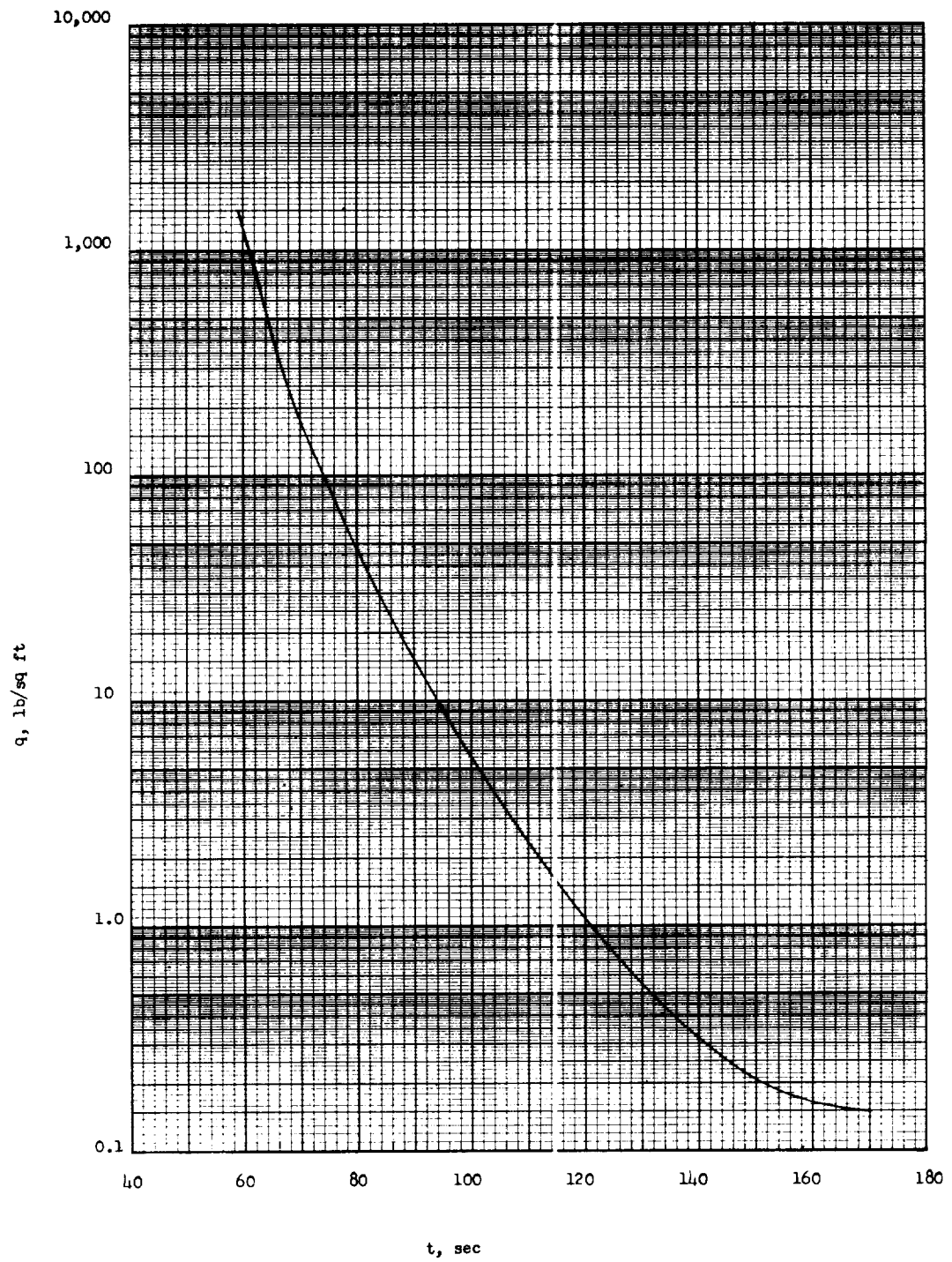


Figure 4.- Dynamic pressure as a function of flight time during coasting flight.

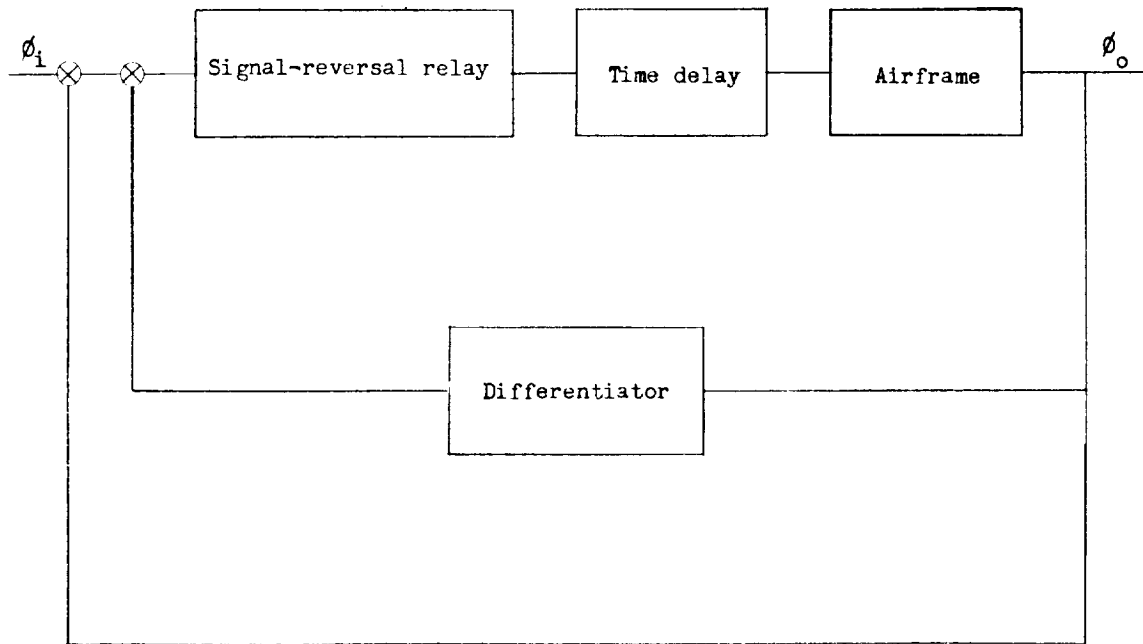
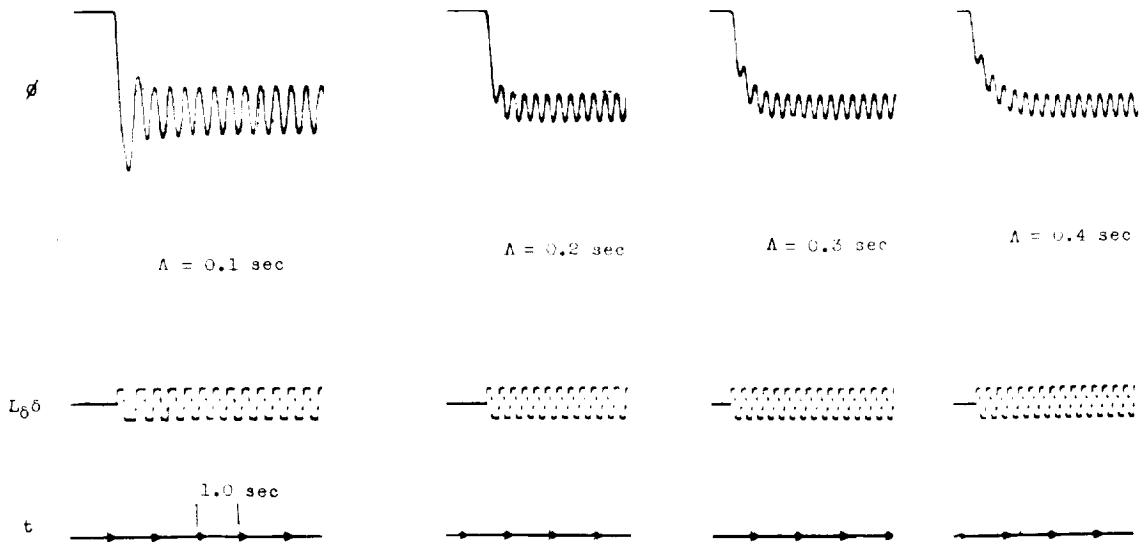
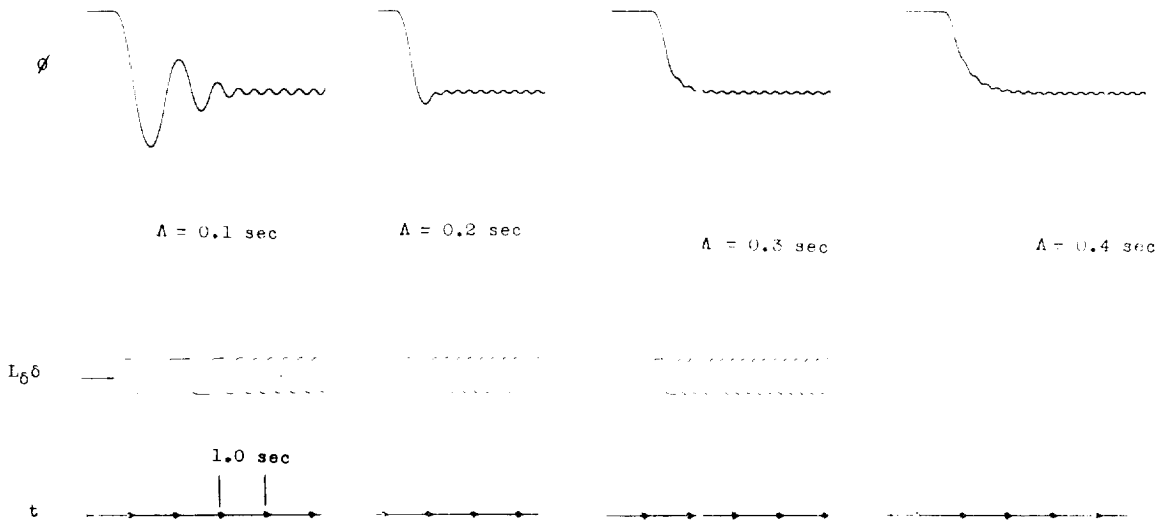


Figure 5.- Simplified block diagram of flicker displacement-plus-rate control.



(a)  $t = 50$  seconds;  $h = 82,000$  feet;  $V = 6,100$  ft/sec.



(b)  $t = 70$  seconds;  $h = 123,000$  feet;  $V = 5,800$  ft/sec.

Figure 6.- Effect of rate factor on roll response at various flight times.  $\phi_i = 10^\circ$ ;  $\tau = 0.04$  second;  $\delta = \pm 5^\circ$ ;  $L_0 = 0$ ; actual value of  $L_p$ .

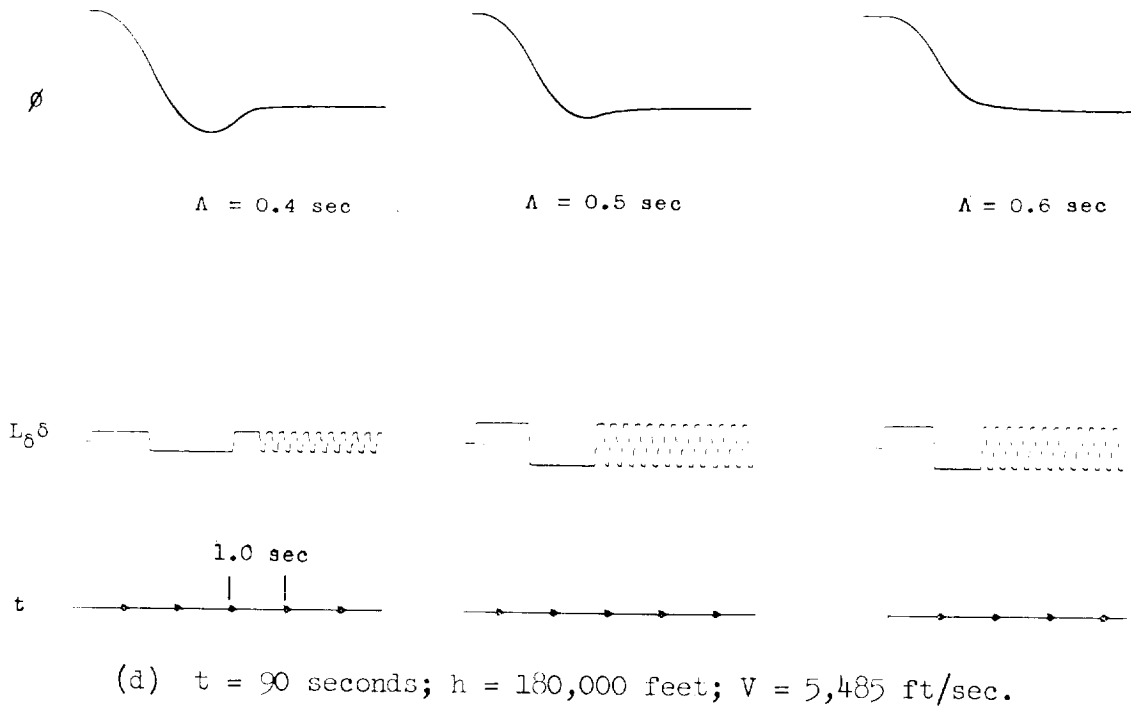
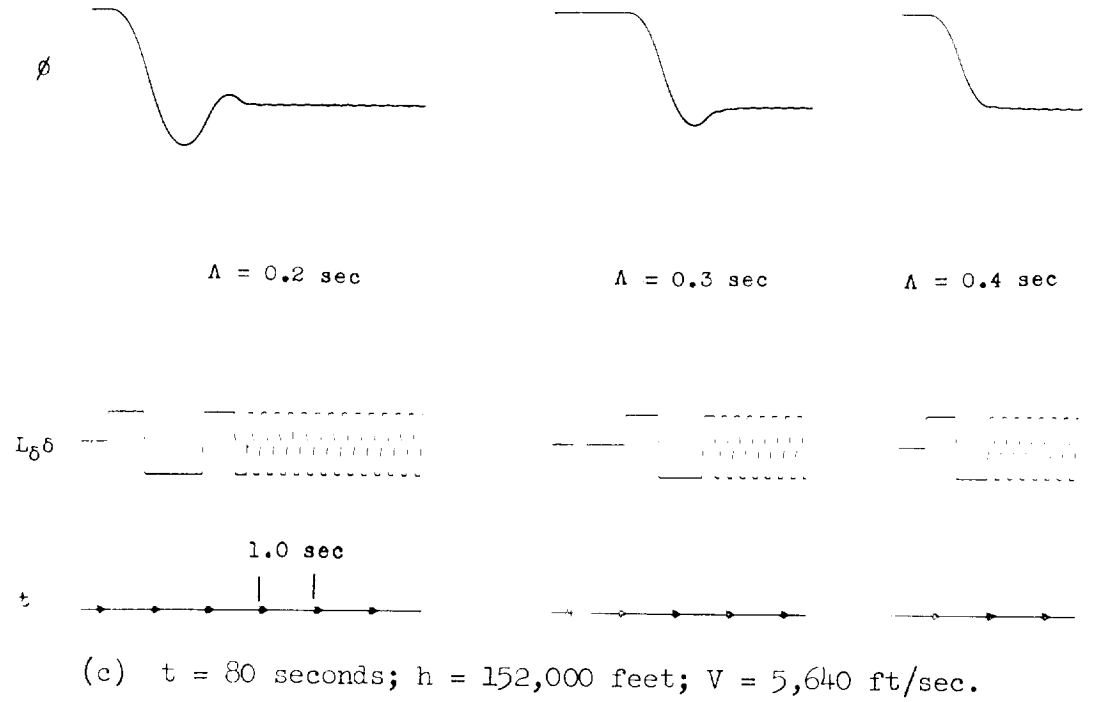
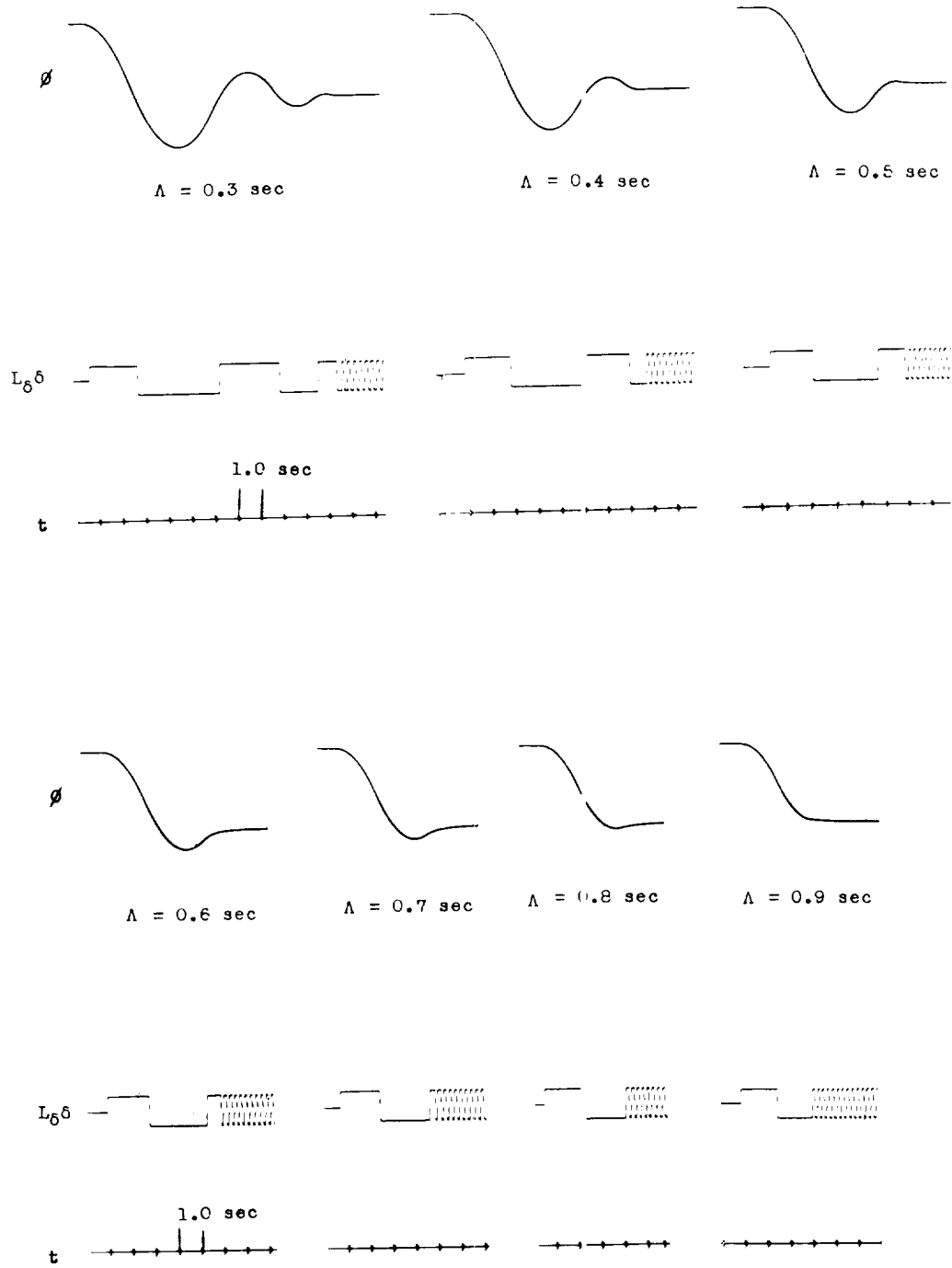
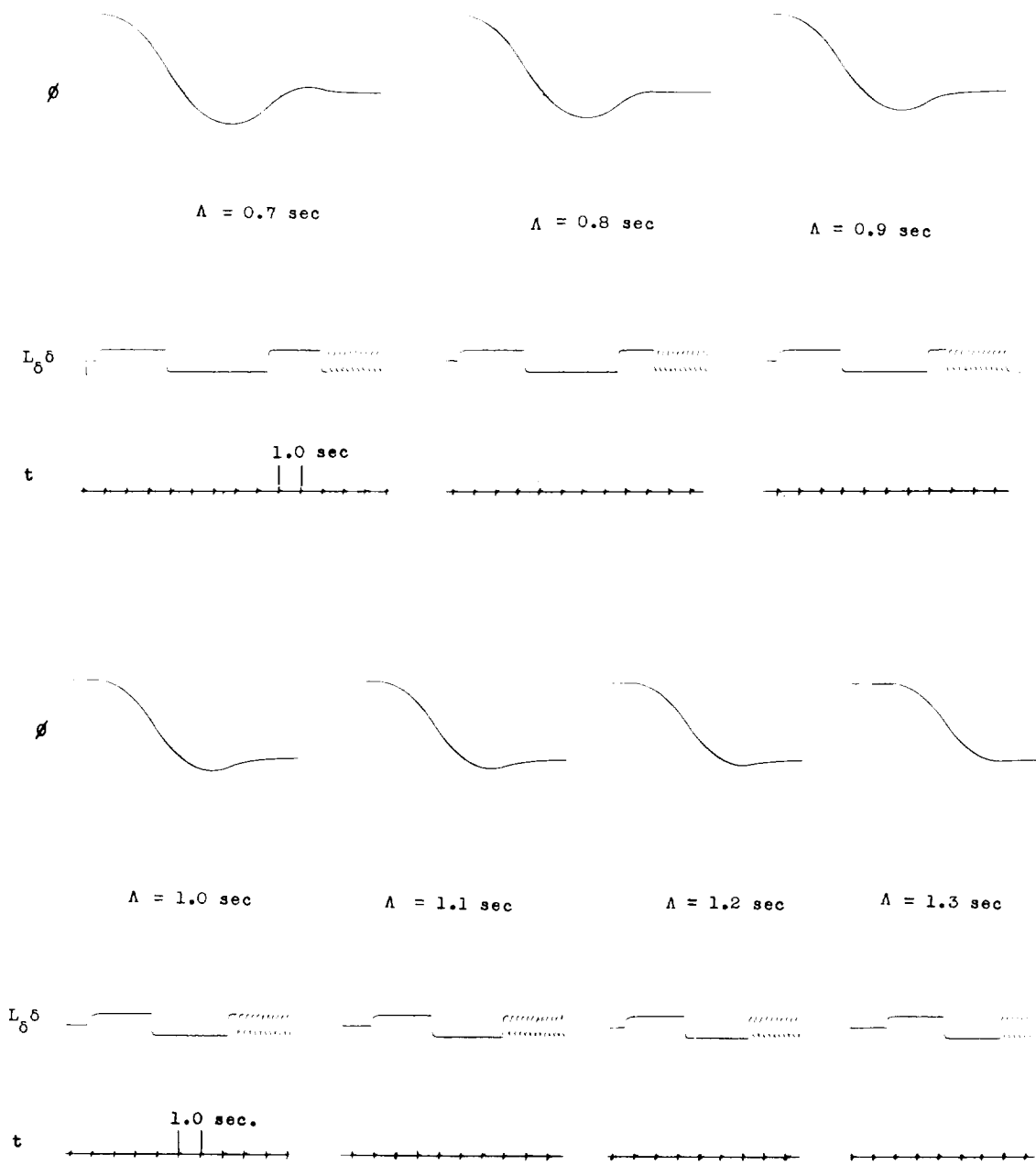


Figure 6.- Continued.



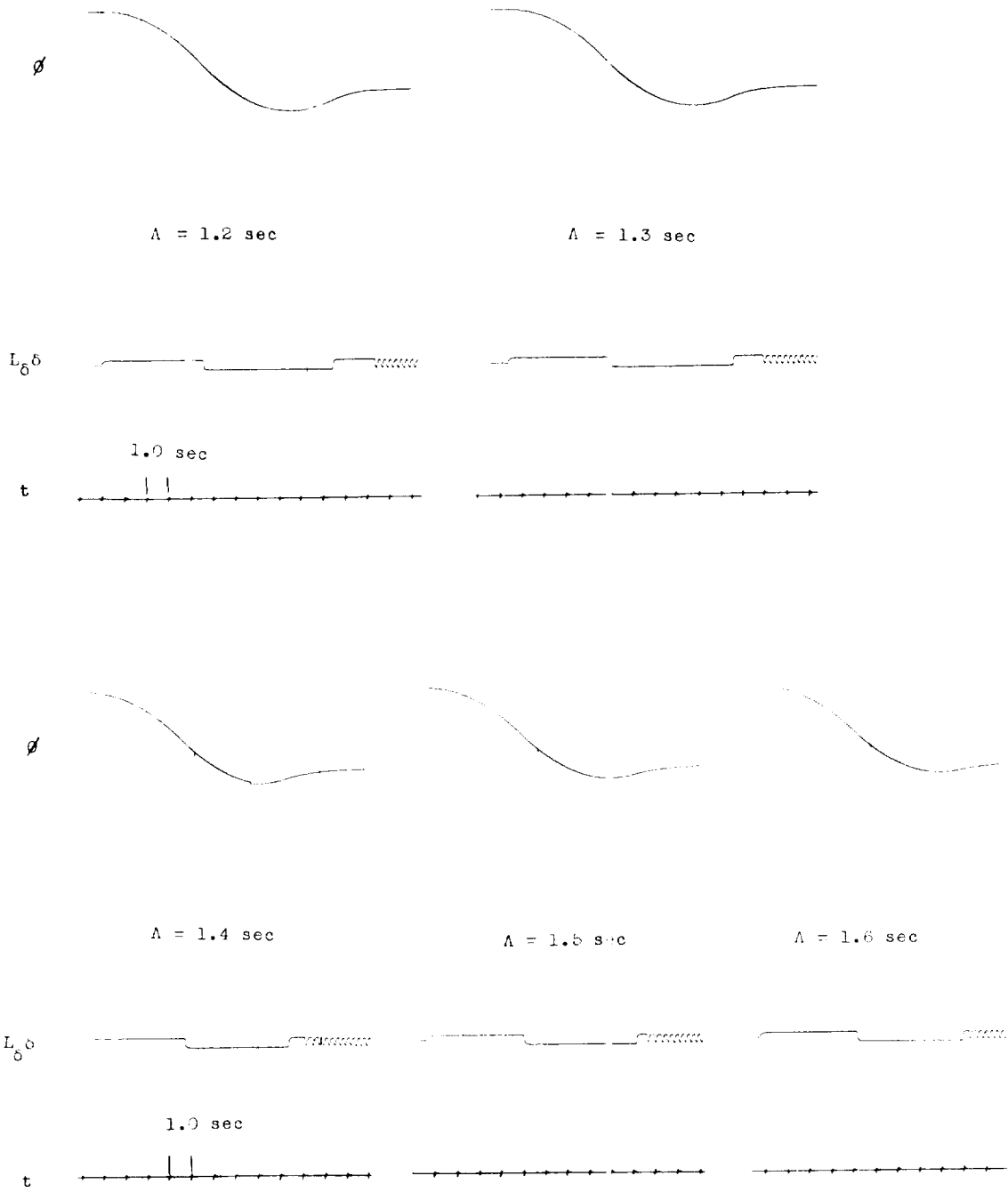
(e)  $t = 100$  seconds;  $h = 204,000$  feet;  $V = 5,340$  ft/sec.

Figure 6.- Continued.



(f)  $t = 110$  seconds;  $h = 225,000$  feet;  $V = 5,210$  ft/sec.

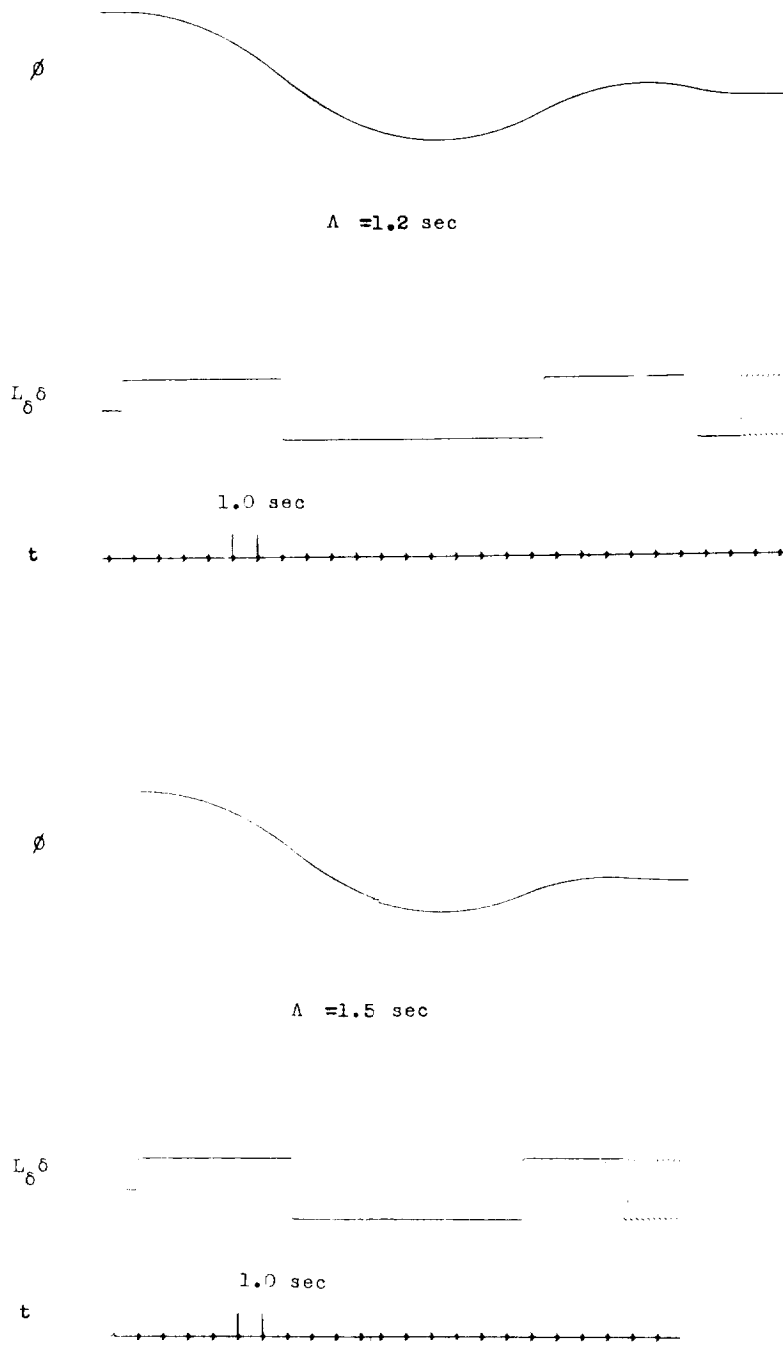
Figure 6.- Continued.



(g)  $t = 120$  seconds;  $h = 243,000$  feet;  $V = 5,100$  ft/sec.

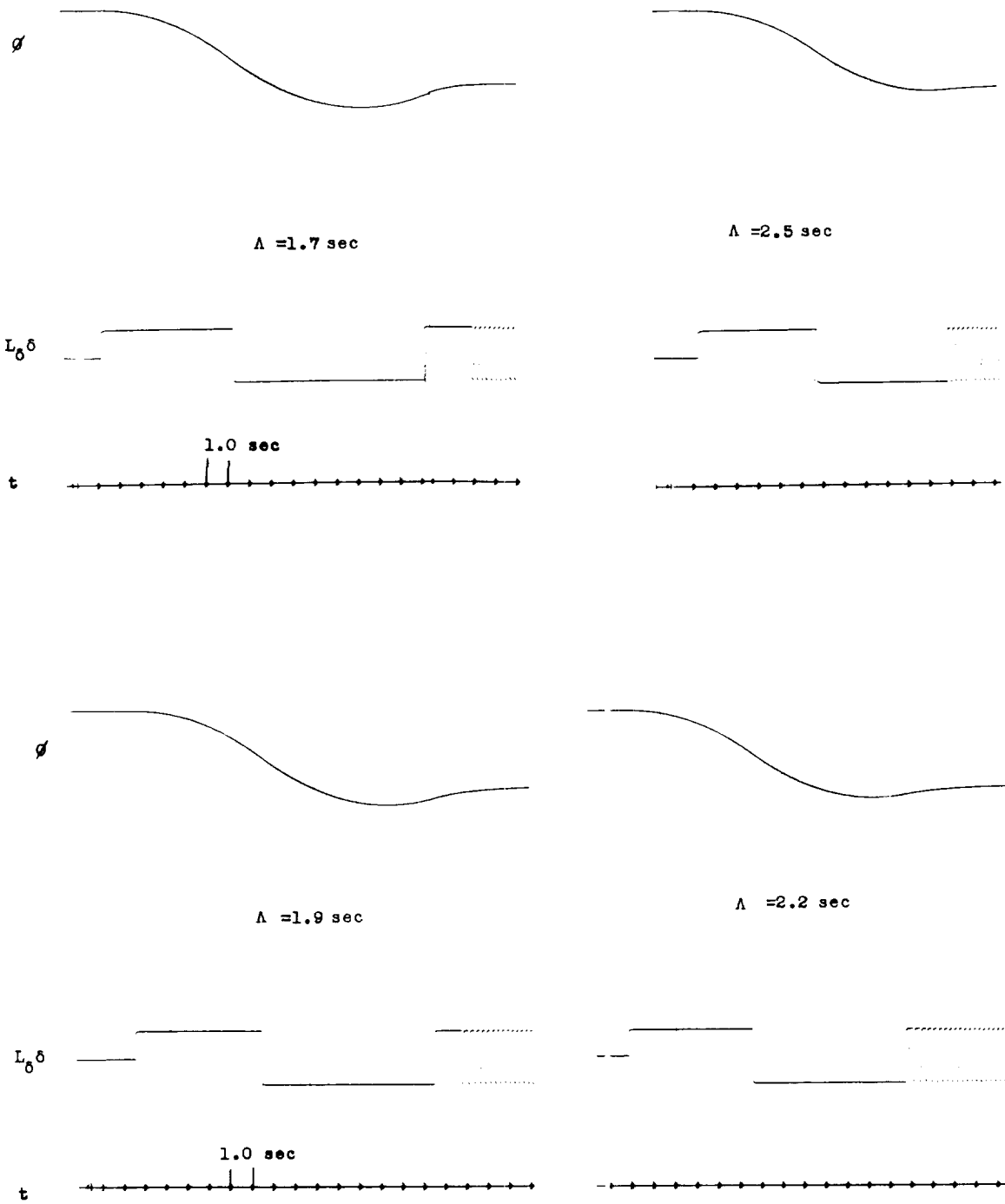
Figure 6.- Continued.





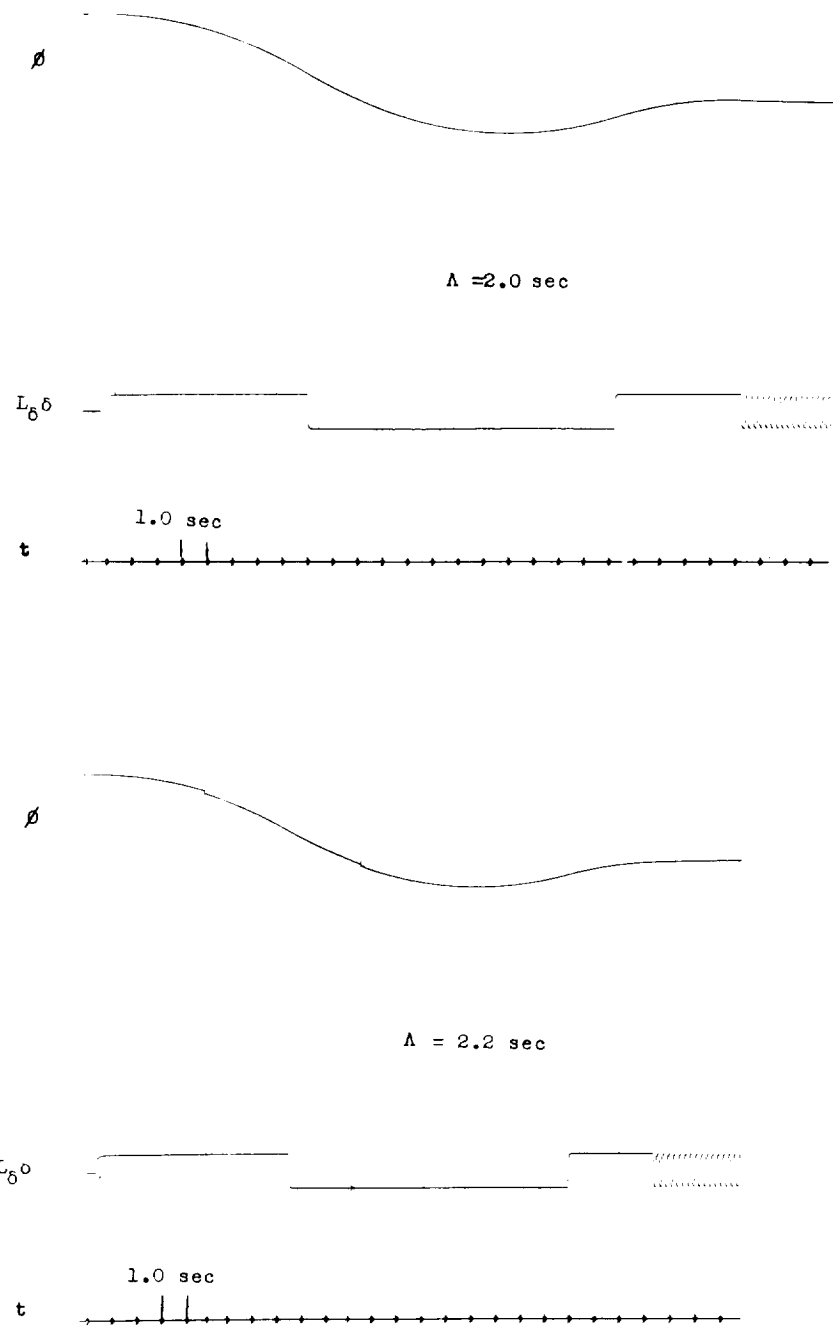
(h)  $t = 130$  seconds;  $h = 257,000$  feet;  $V = 5,005$  ft/sec.

Figure 6.- Continued.



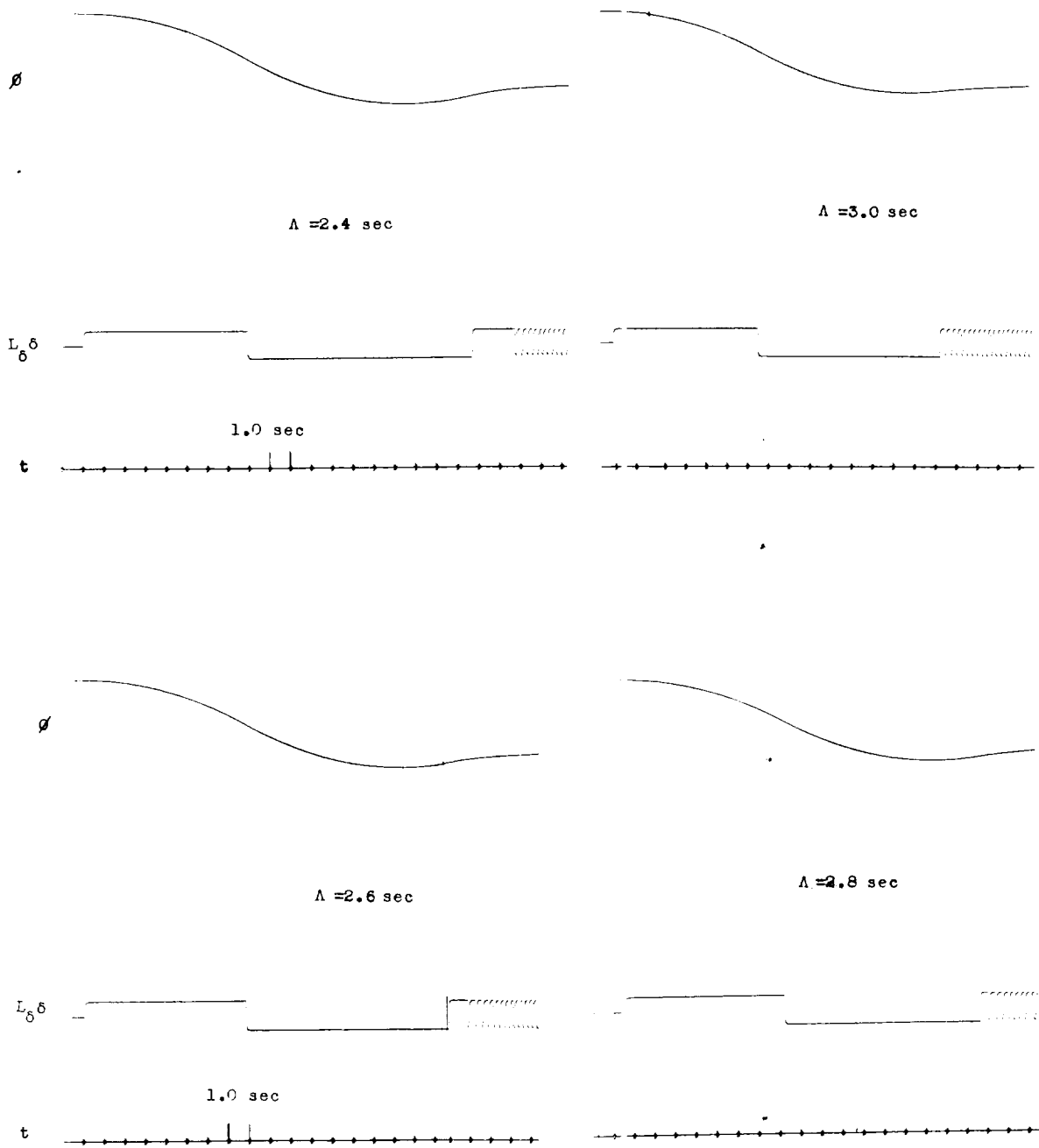
(h) Concluded.

Figure 6.- Continued.



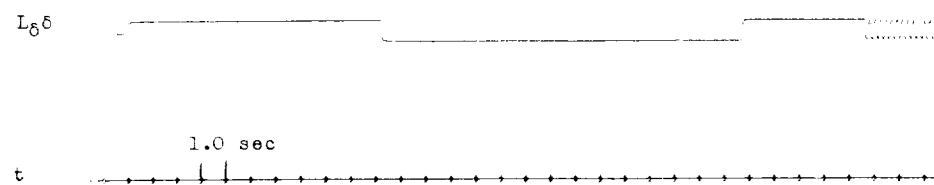
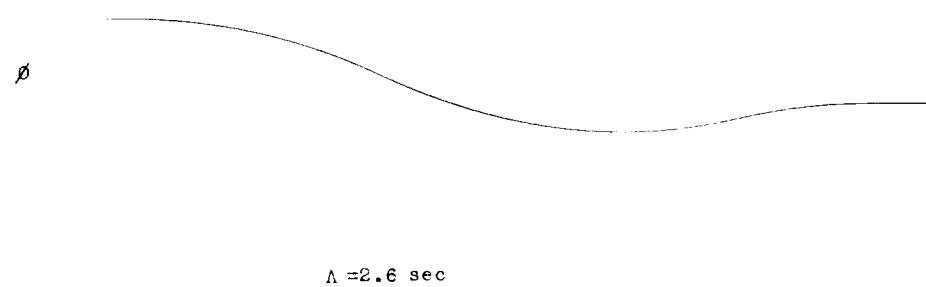
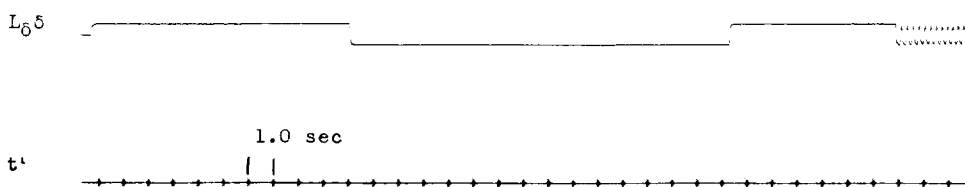
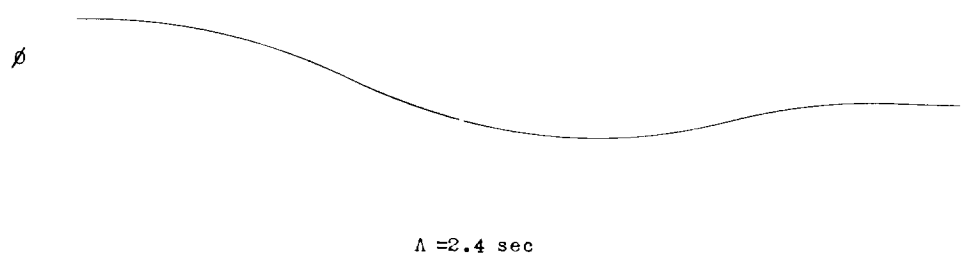
(i)  $t = 140$  seconds;  $h = 268,000$  feet;  $V = 4,930$  ft/sec.

Figure 6.- Continued.



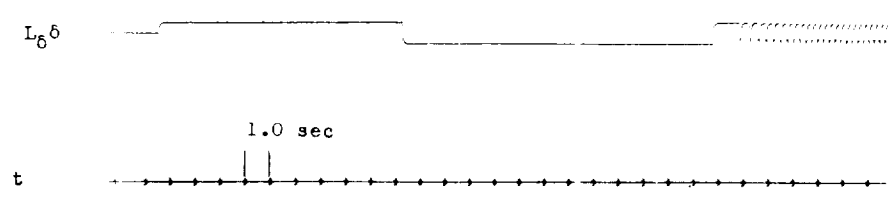
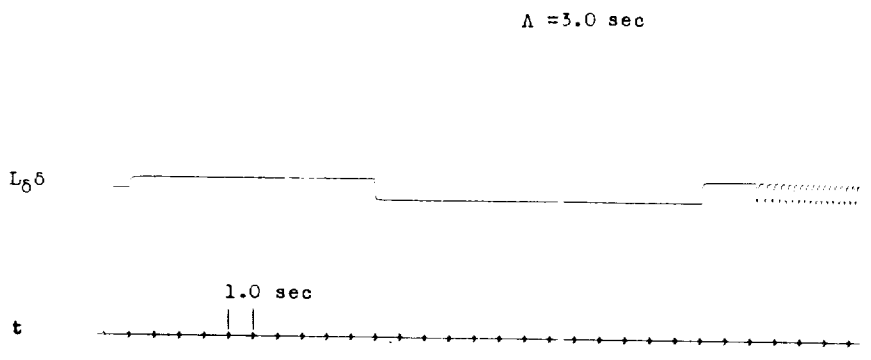
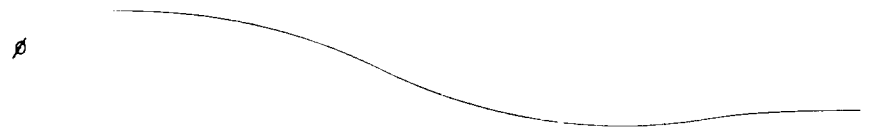
(i) Concluded.

Figure 6.- Continued.



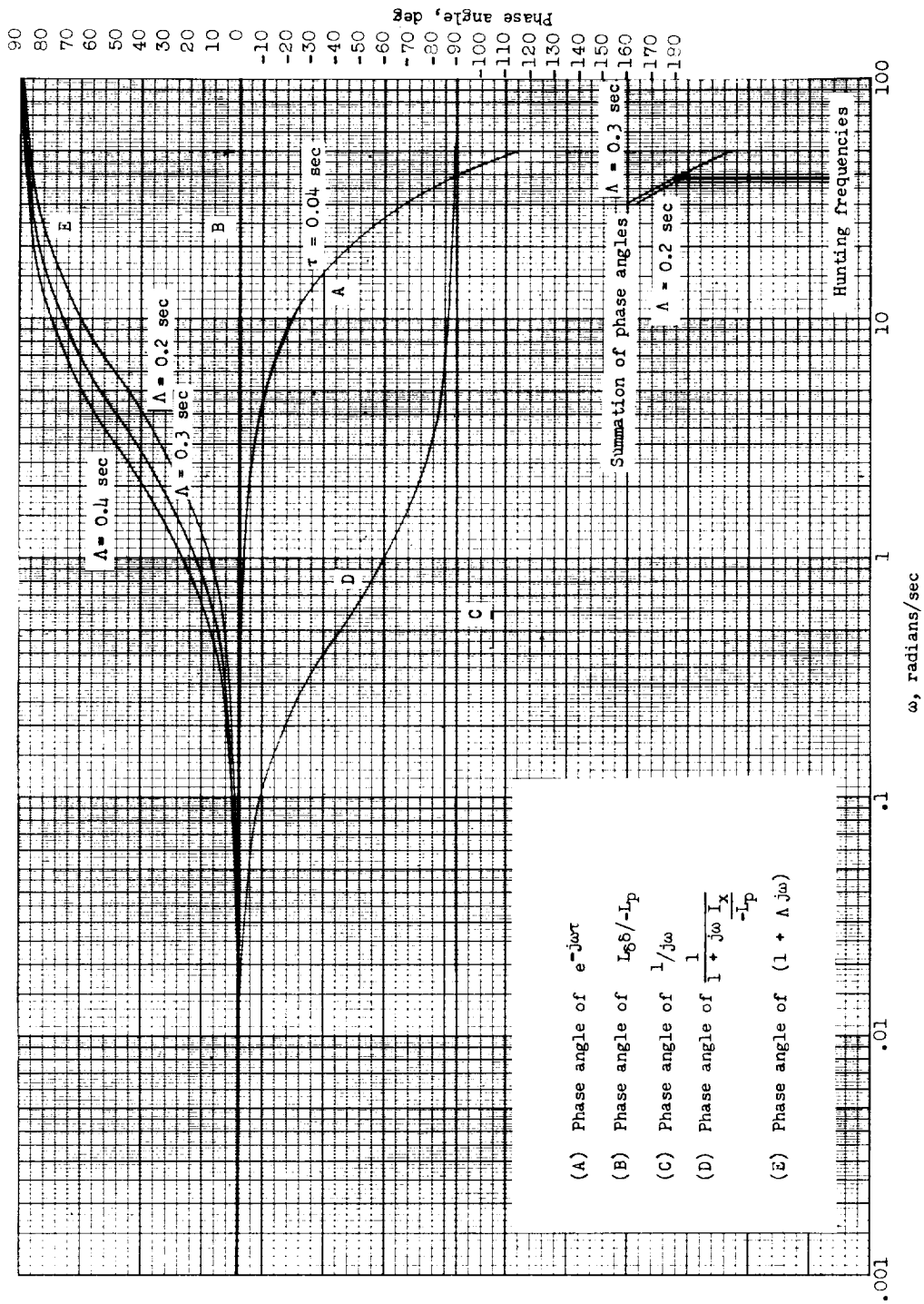
(j)  $t = 150 \text{ seconds}$ ;  $h = 276,000 \text{ feet}$ ;  $V = 4,880 \text{ ft/sec}$ .

Figure 6.- Continued.



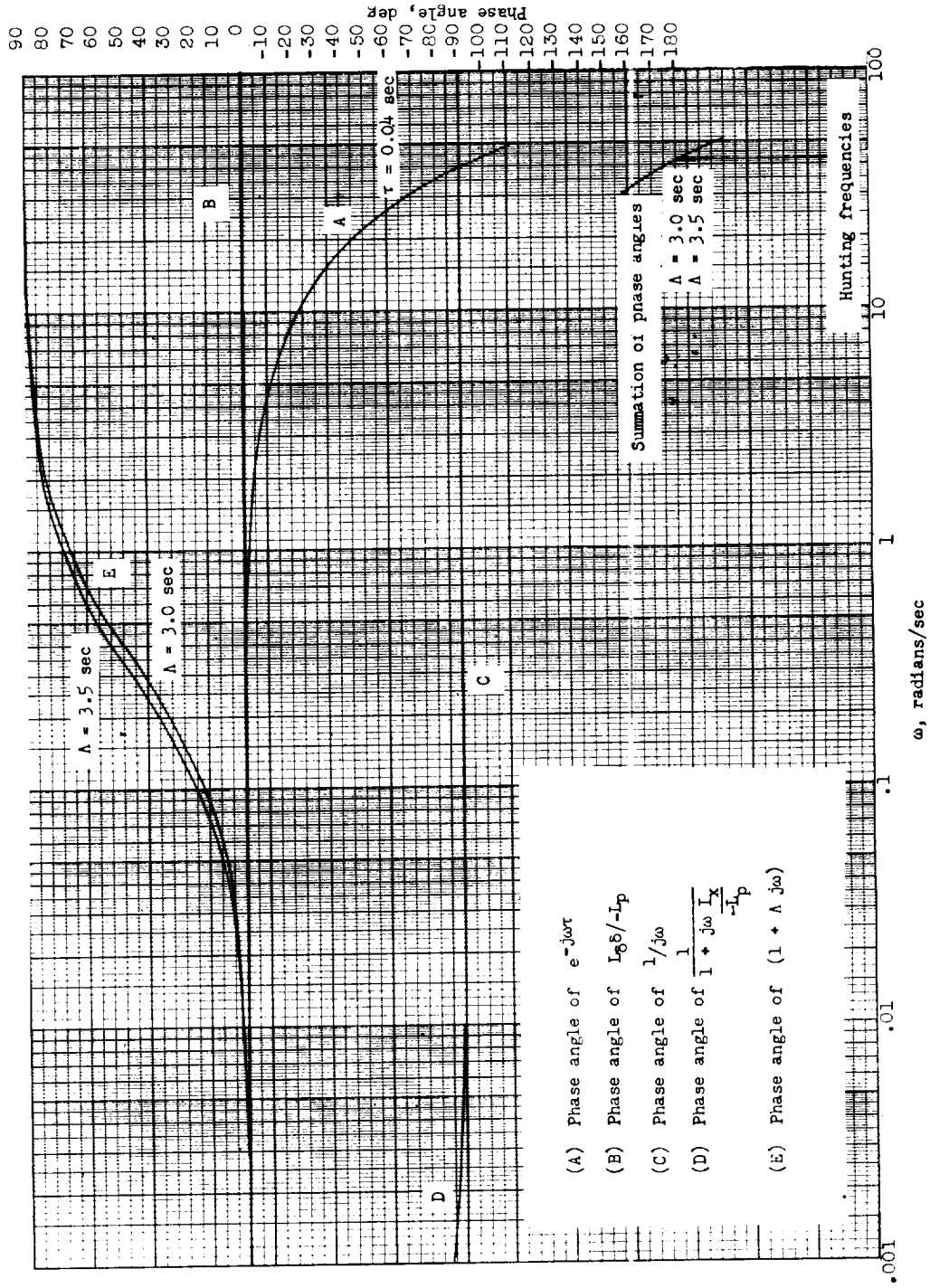
(j) Concluded.

Figure 6.- Concluded.



(a) Phase angle plot at  $t = 59$  seconds,  $h = 82,000$  feet, and  $V = 6,100$  ft/sec.

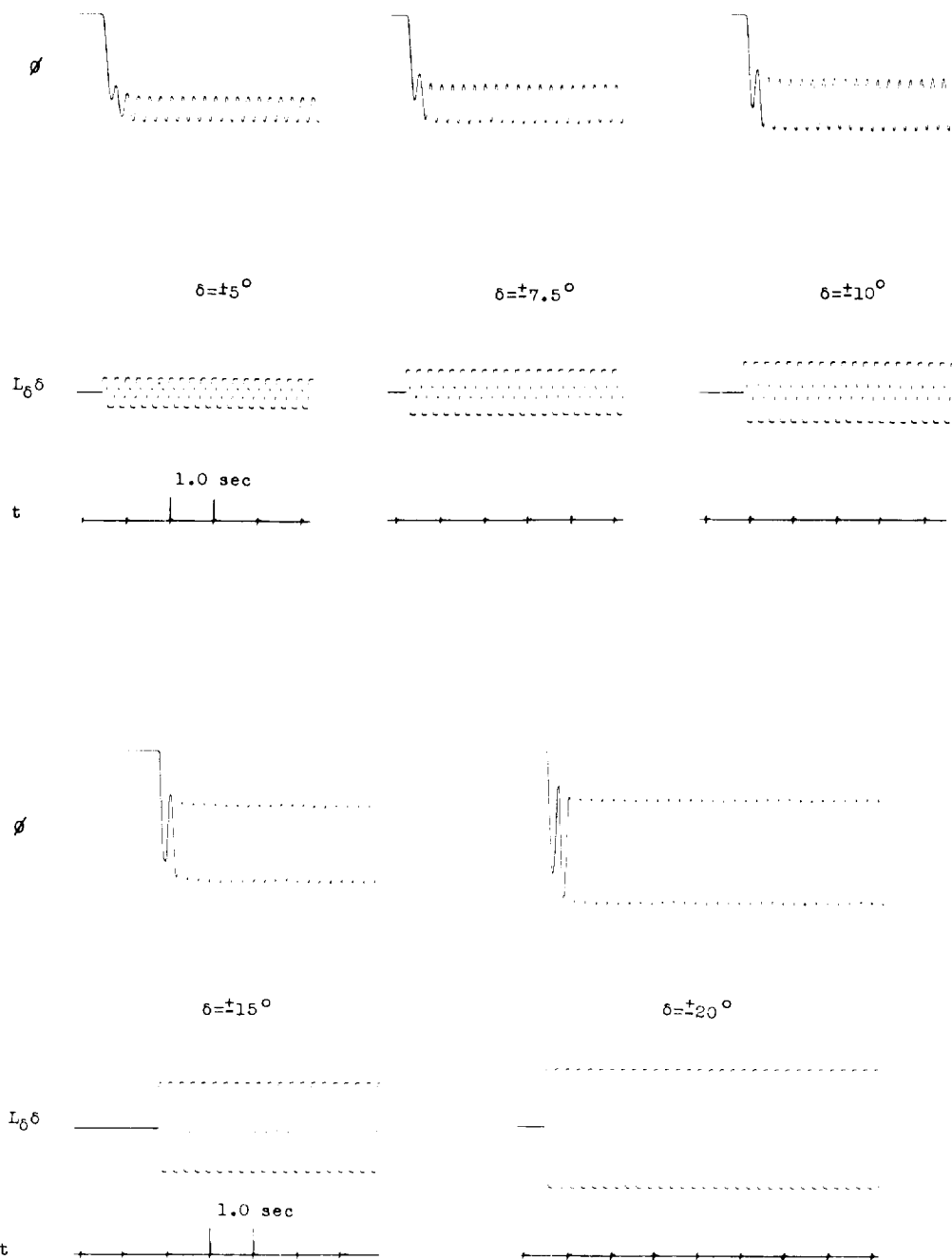
Figure 7.- Calculated phase angles for roll-control system.  $\delta = \pm 5^\circ$ ; actual value of  $L_p$ .



(b) Phase angle plot at  $t = 170$  seconds,  $h = 282,000$  feet, and  $V = 4,830$  ft/sec.

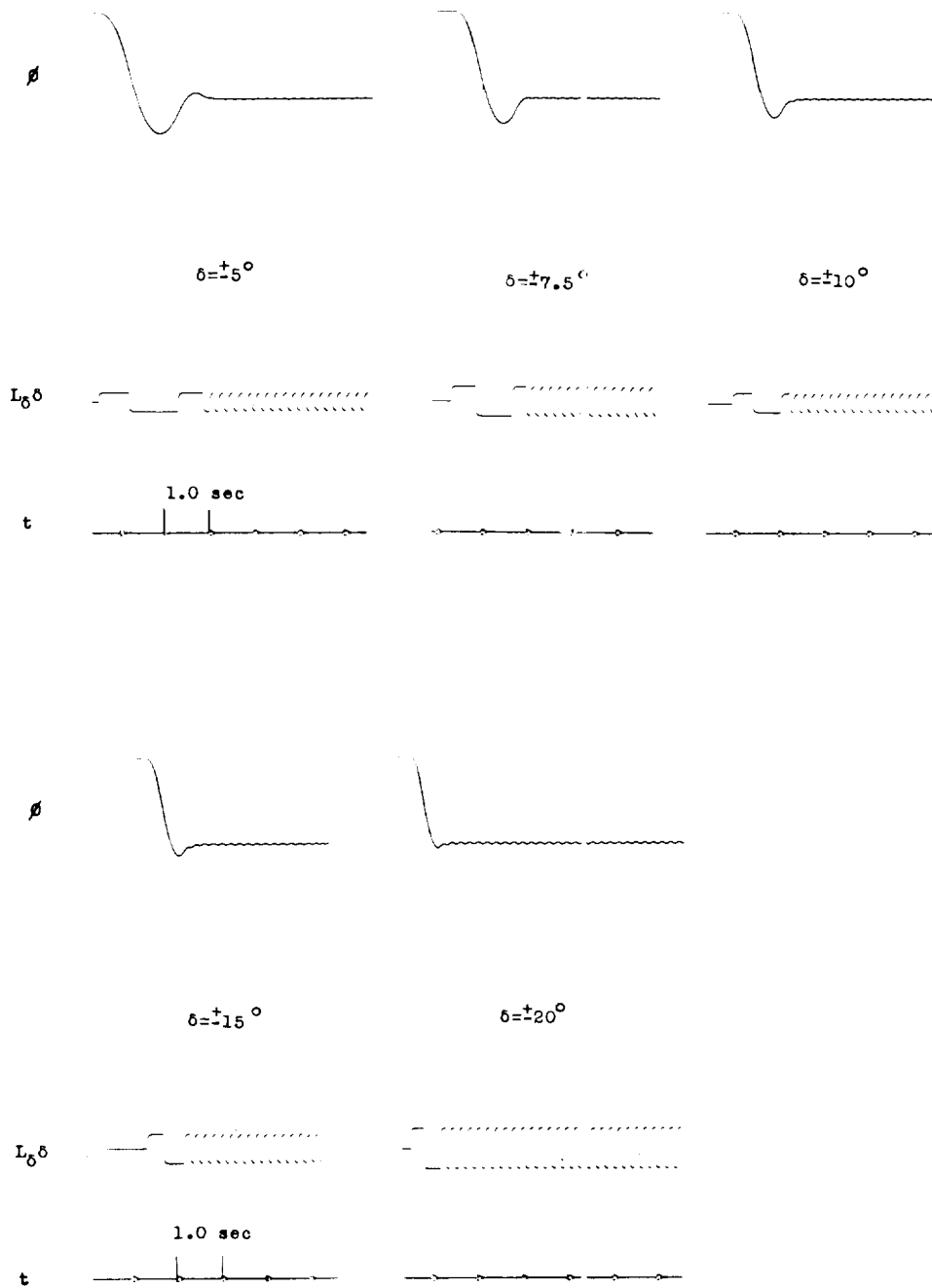
Figure 7.- Concluded.





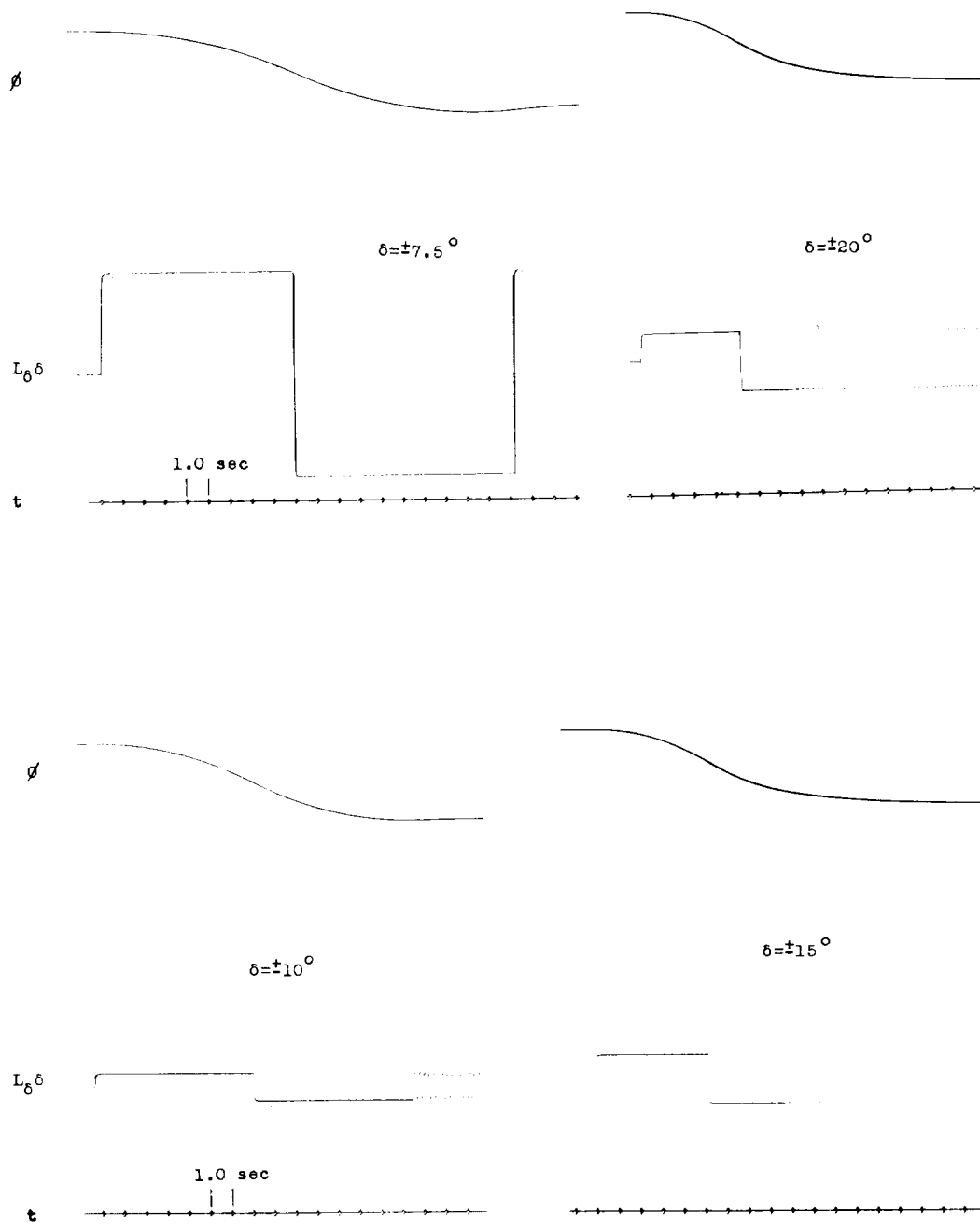
(a)  $t = 59$  seconds;  $h = 82,000$  feet;  $V = 6,100$  ft/sec;  $\Lambda = 0.2$  second.

Figure 8.- Effect of control moment on the roll response.  $\phi_i = 10^\circ$ ;  
 $\tau = 0.04$  second;  $L_0 = 0$ ; actual value of  $L_p$ .



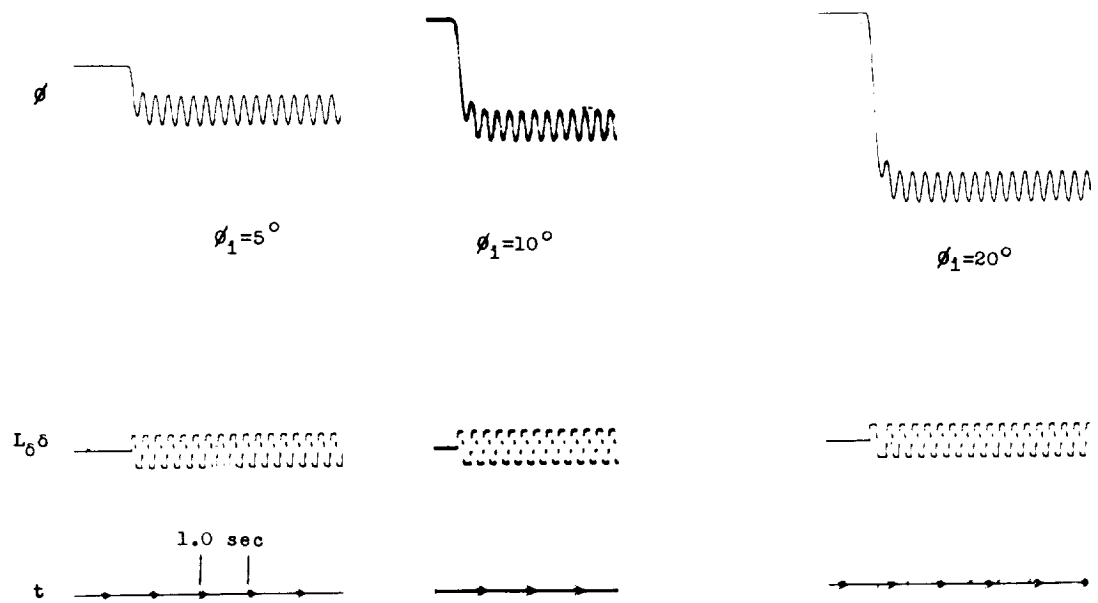
(b)  $t = 80$  seconds;  $h = 152,000$  feet;  $V = 5,640$  ft/sec;  $\Lambda = 0.2$  second.

Figure 8.- Continued.

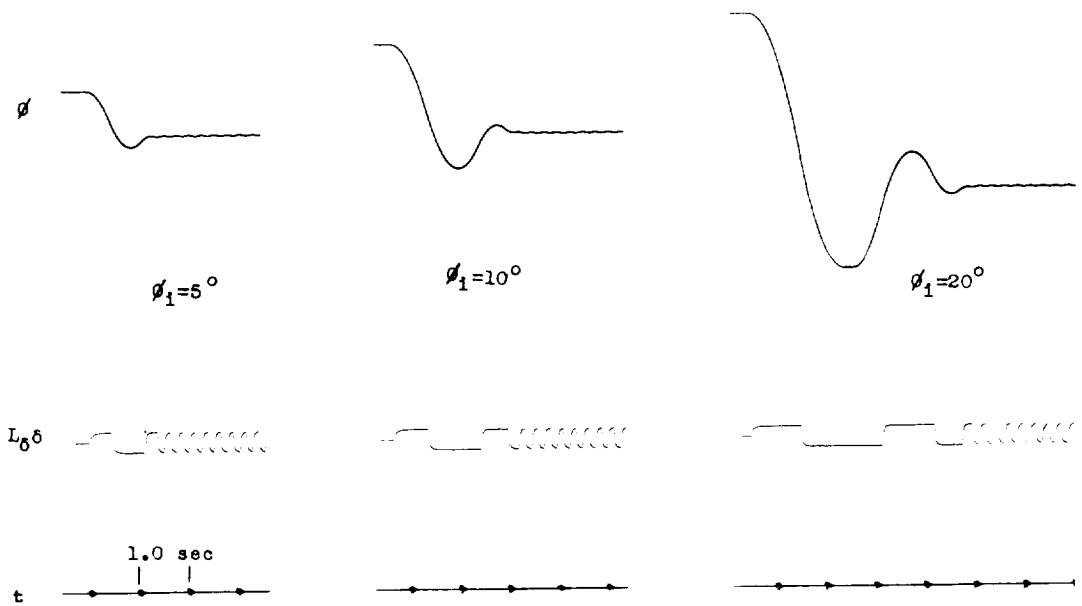


(c)  $t = 170$  seconds;  $h = 282,000$  feet;  $V = 4,830$  ft/sec;  $\Lambda = 3.5$  seconds.

Figure 8.- Concluded.

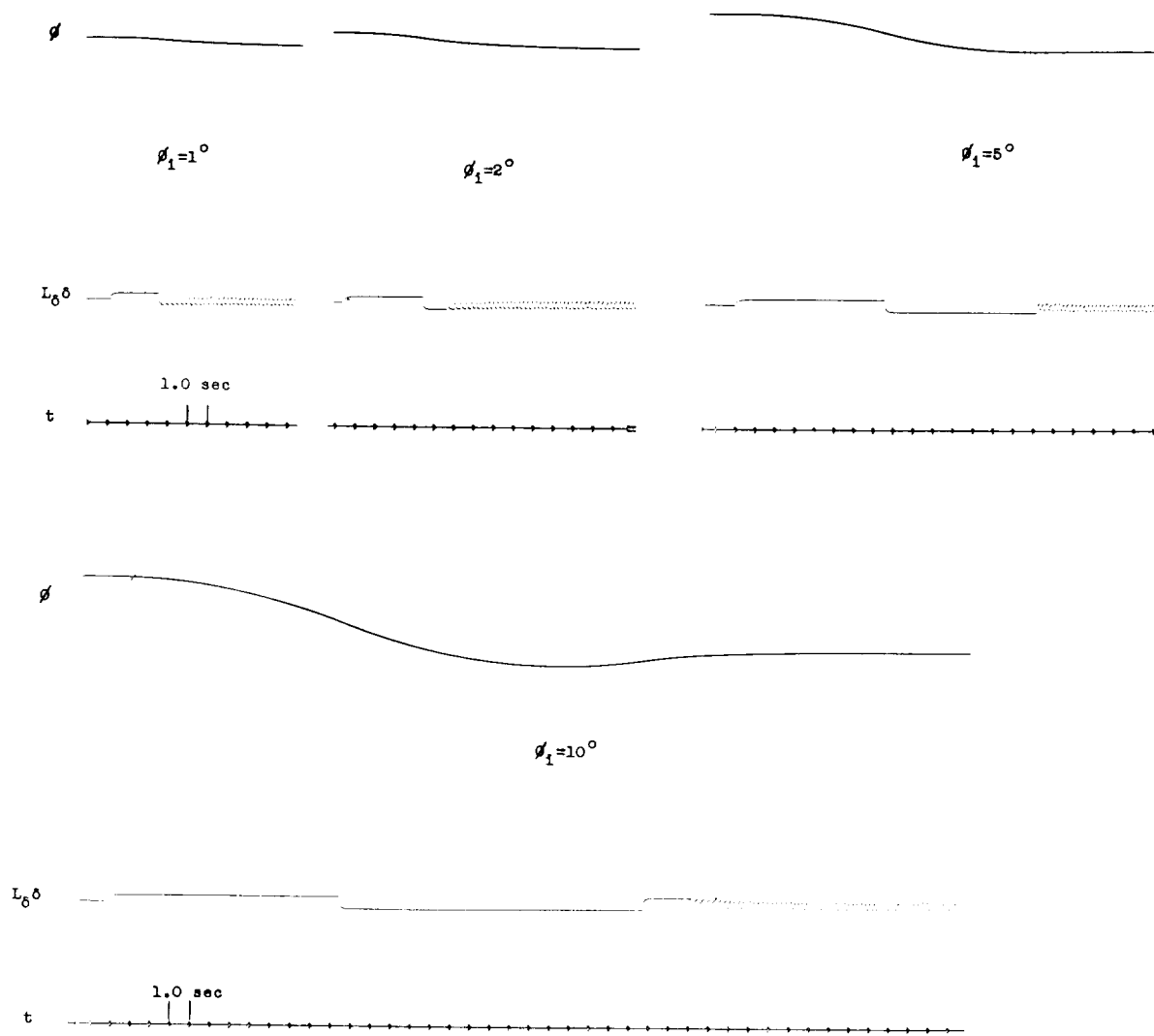


(a)  $t = 59$  seconds;  $h = 82,000$  feet;  $V = 6,100$  ft/sec;  $\Lambda = 0.2$  second.



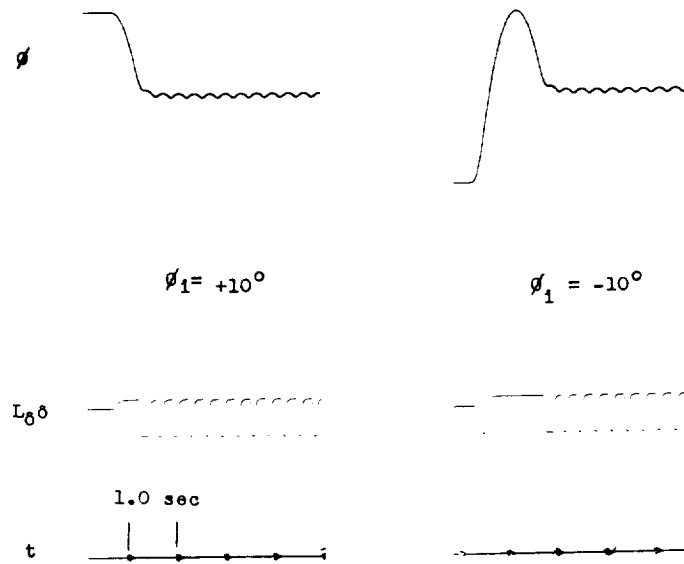
(b)  $t = 80$  seconds;  $h = 152,000$  feet;  $V = 5,640$  ft/sec;  $\Lambda = 0.2$  second.

Figure 9.- Effect of magnitude of disturbance on roll response.  $\delta = \pm 5^\circ$ ;  $\tau = 0.04$  second;  $L_0 = 0$ ; actual value of  $L_p$ .

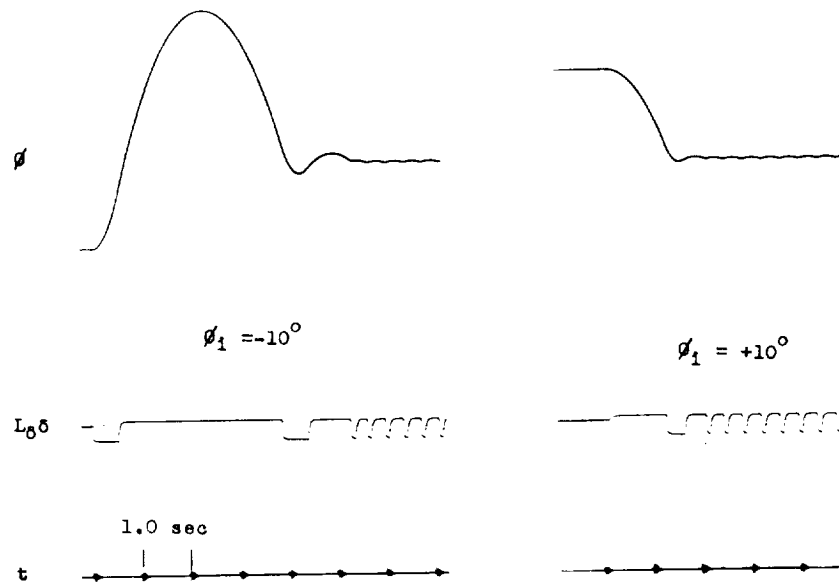


(c)  $t = 170$  seconds;  $h = 282,000$  feet;  $V = 4,830$  ft/sec;  $\Lambda = 3.5$  seconds.

Figure 9.- Concluded.



(a)  $t = 70$  seconds;  $h = 123,000$  feet;  $V = 5,800$  ft/sec.



(b)  $t = 80$  seconds;  $h = 152,000$  feet;  $V = 5,640$  ft/sec.

Figure 10.- Effect of asymmetry at  $t = 70$  seconds and  $t = 80$  seconds.  
 $\tau = 0.04$  second;  $\Lambda = 0.2$  second;  $L_0 = 2.5L_6$ ;  $\delta = \pm 5^\circ$ ; actual value  
of  $L_p$ .

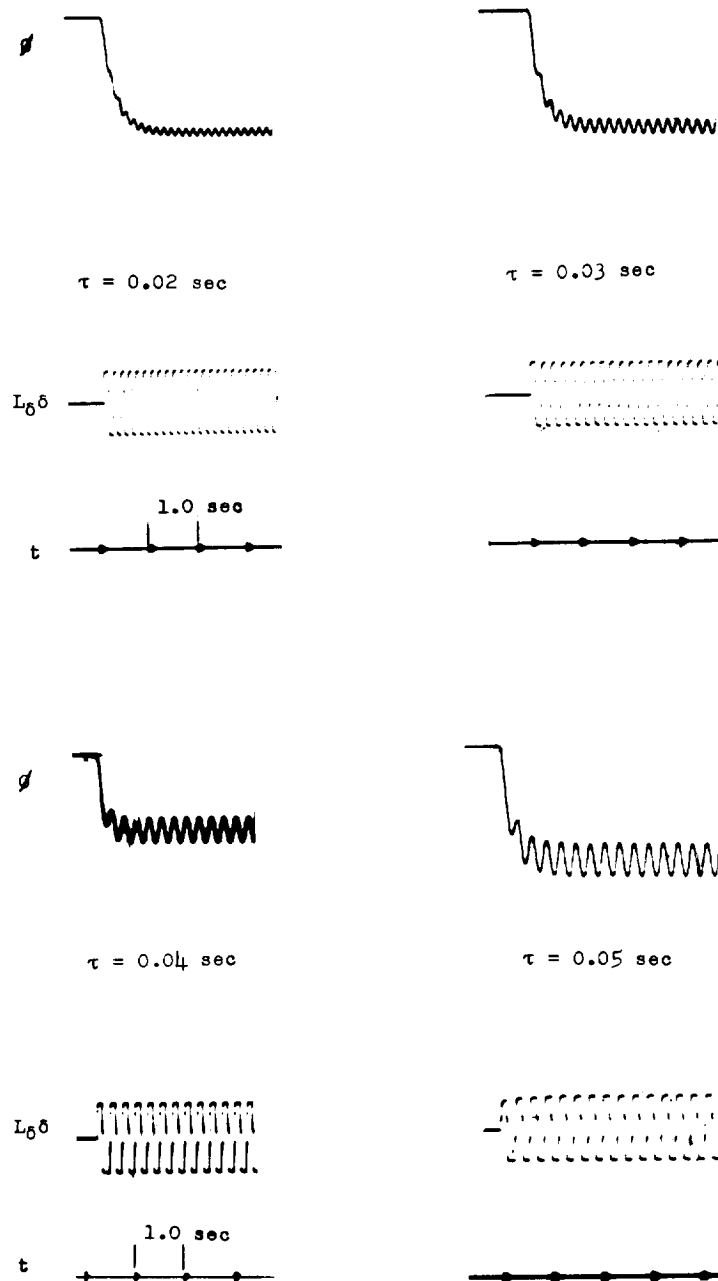
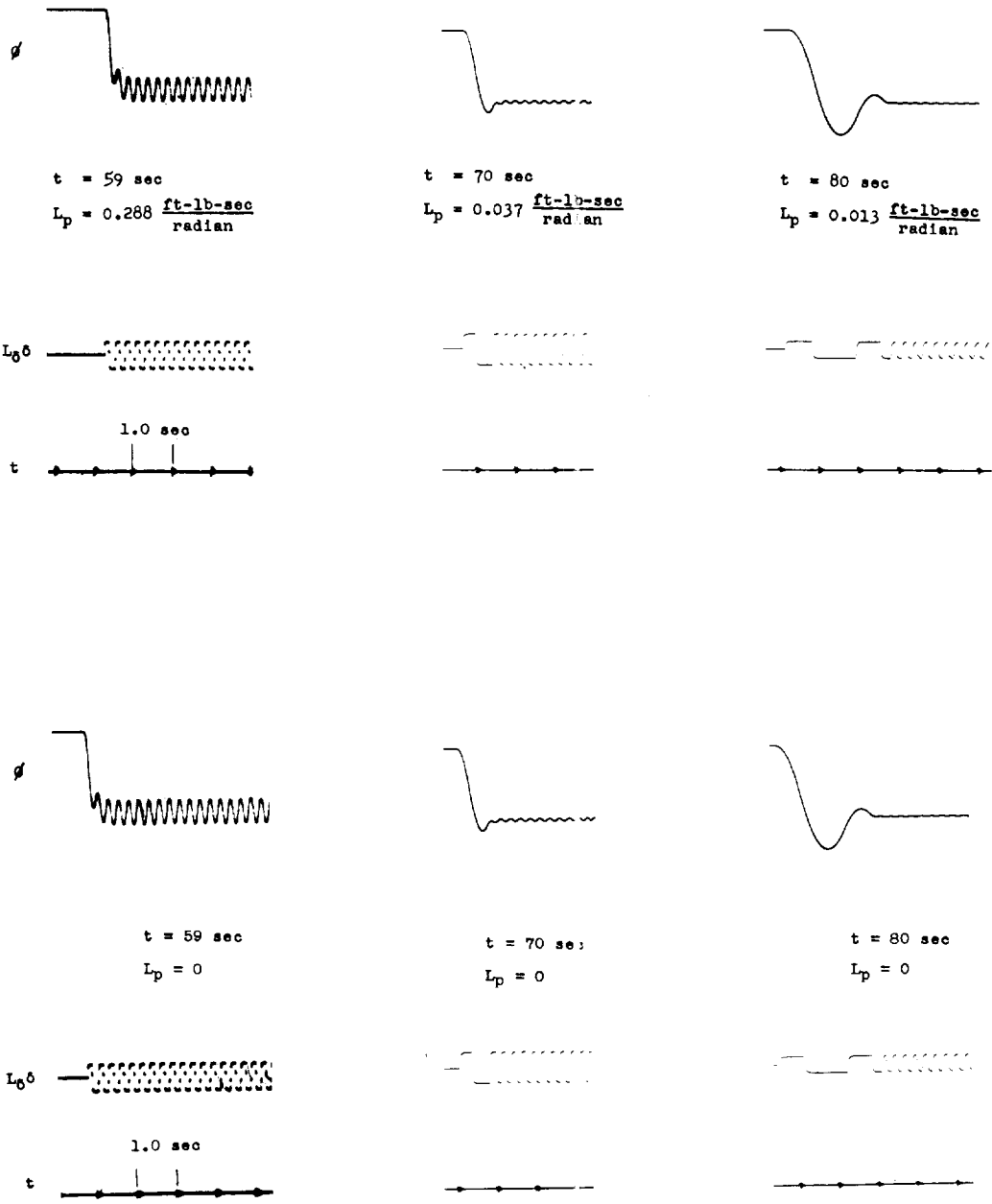


Figure 11.- Effect of lag time on roll response.  $t = 59$  seconds;  
 $h = 82,000$  feet;  $V = 6,100$  ft/sec;  $\phi_i = 10^\circ$ ;  $\Lambda = 0.2$  second;  
 $L_0 = 0$ ; actual value of  $L_p$ .



(a)  $t = 59$ ;  $V = 6,100$ ;  $h = 82,000$ ; (b)  $t = 70$ ;  $V = 5,800$ ;  $h = 123,000$ ; (c)  $t = 80$ ;  $V = 5,640$ ;  $h = 152,000$ .

Figure 12.- Effect of aerodynamic damping.  $\phi_i = 10^\circ$ ;  $\tau = 0.04$  second;  $\Lambda = 0.2$  second;  $\delta = \pm 5^\circ$ ;  $L_0 = 0$ .



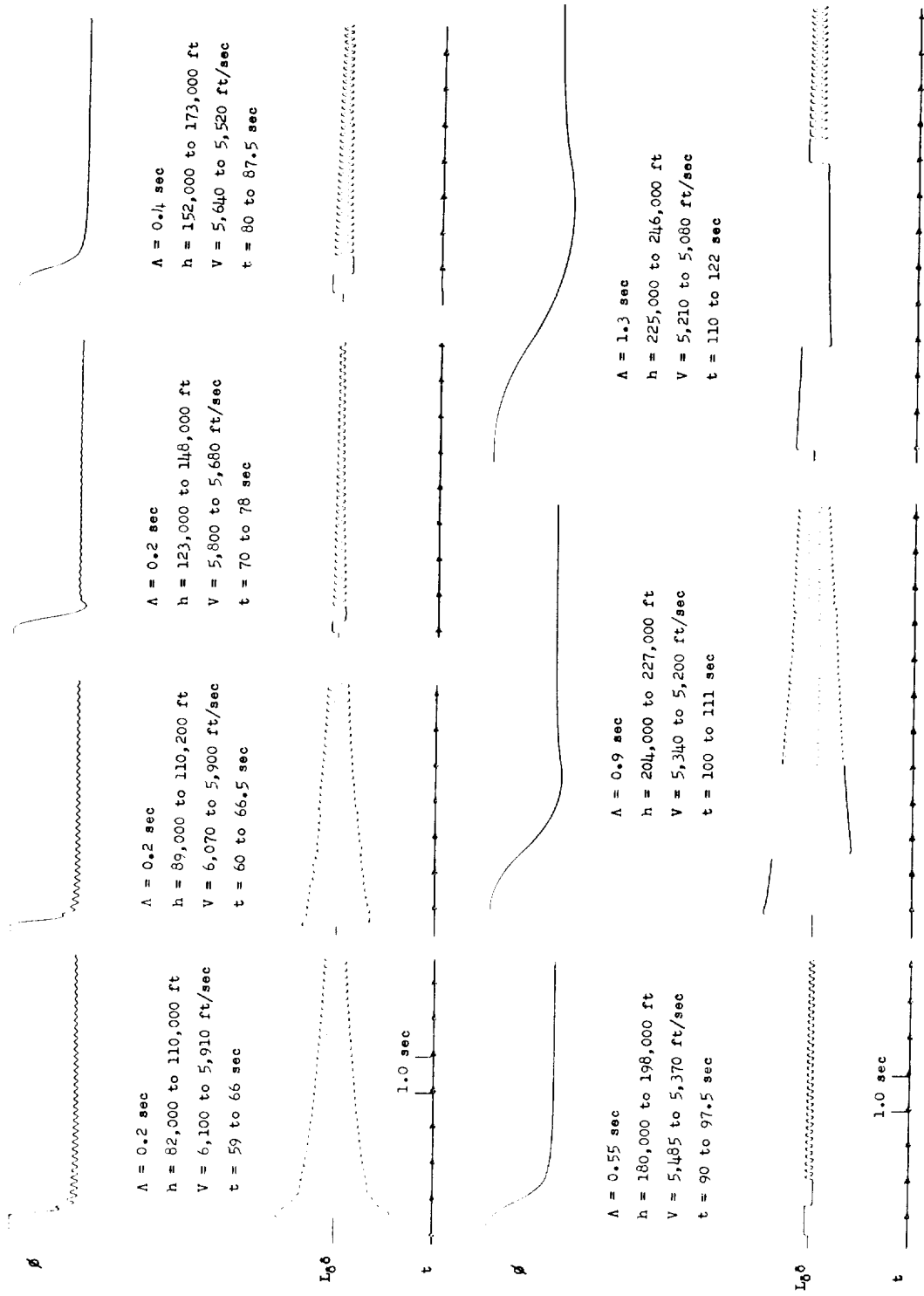


Figure 13.- Roll response of example missile during changing altitude.  $\tau = 0.04$  second;  $\phi_i = 10^\circ$ ;  $\delta = \pm 5^\circ$ ;  $L_0 = 0$ ;  $L_p = 0$ .

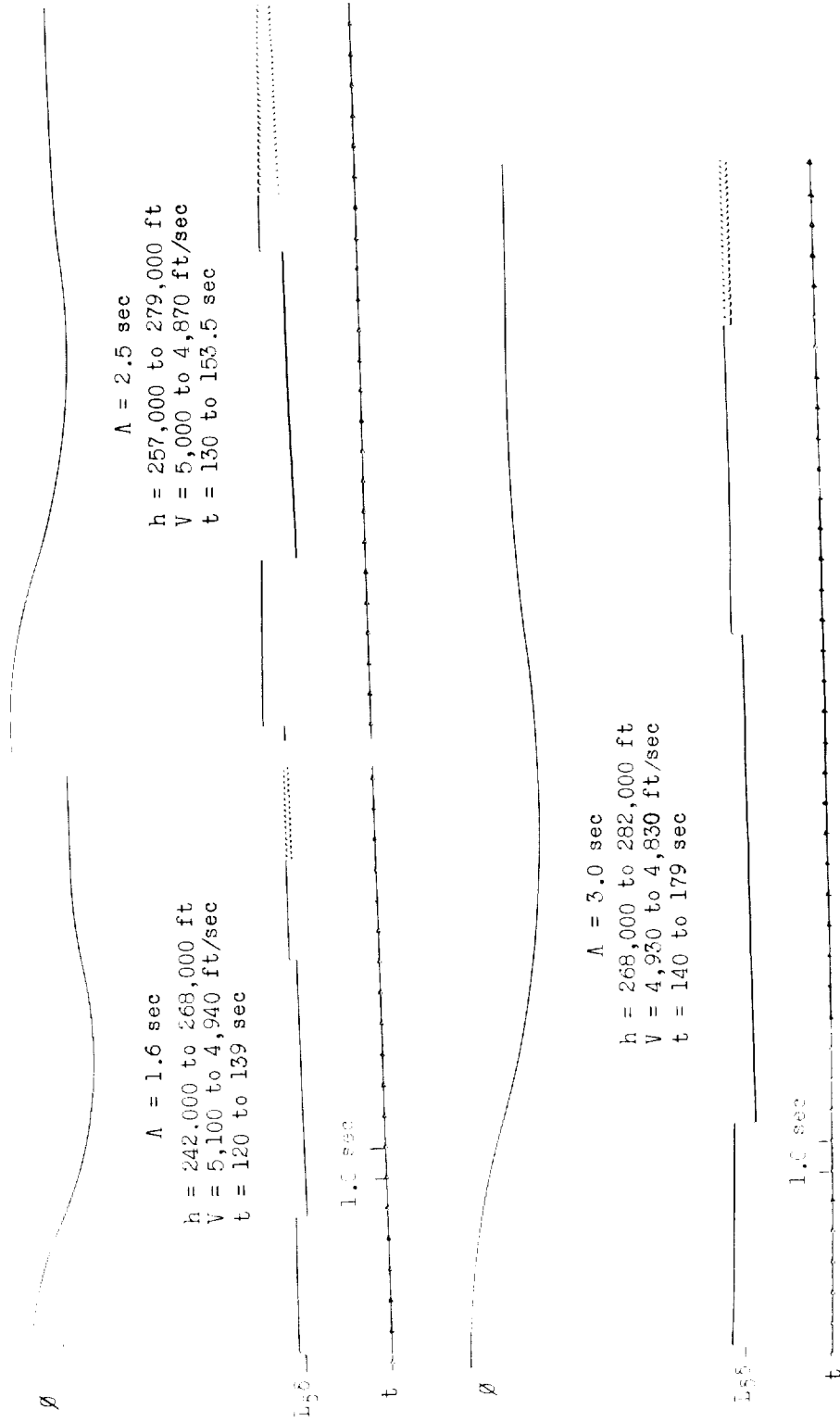


Figure 13.- Continued.

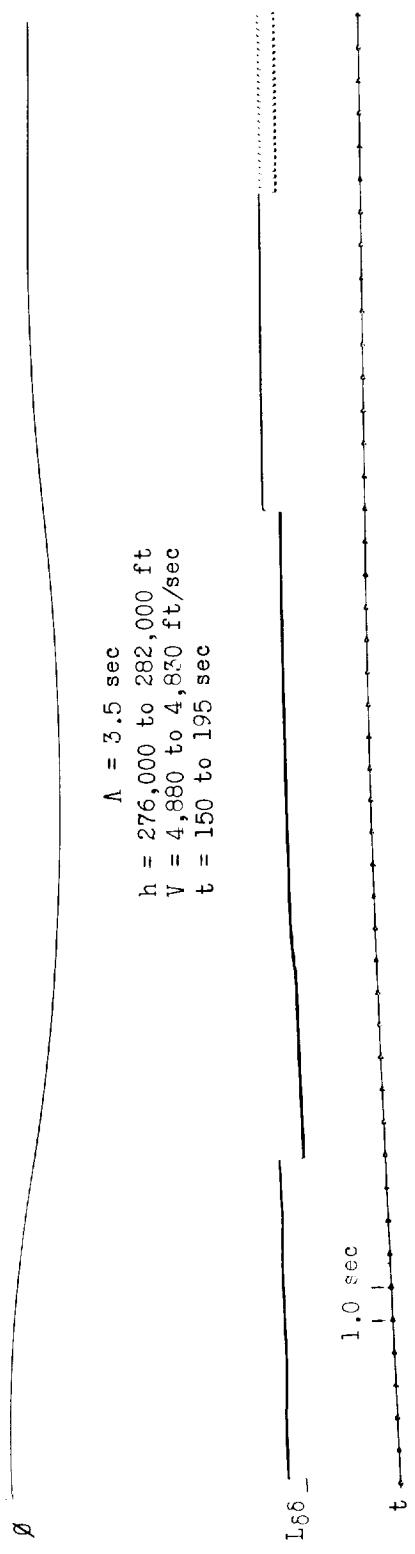
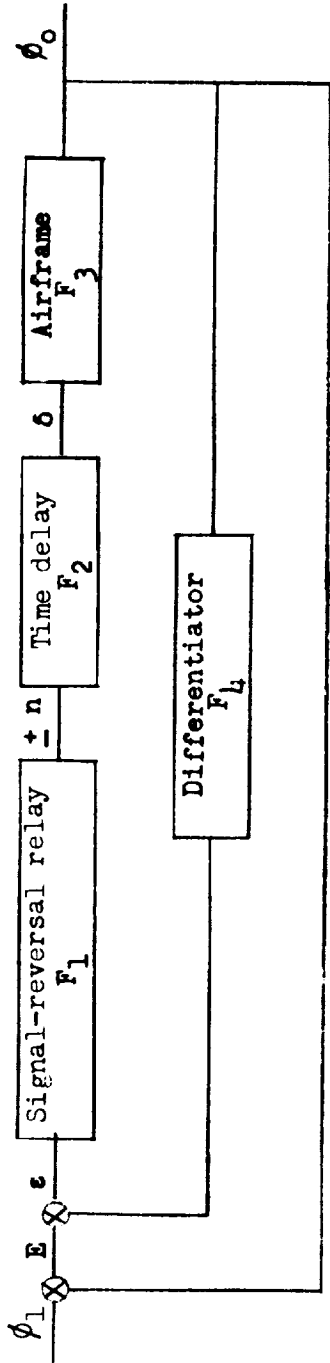
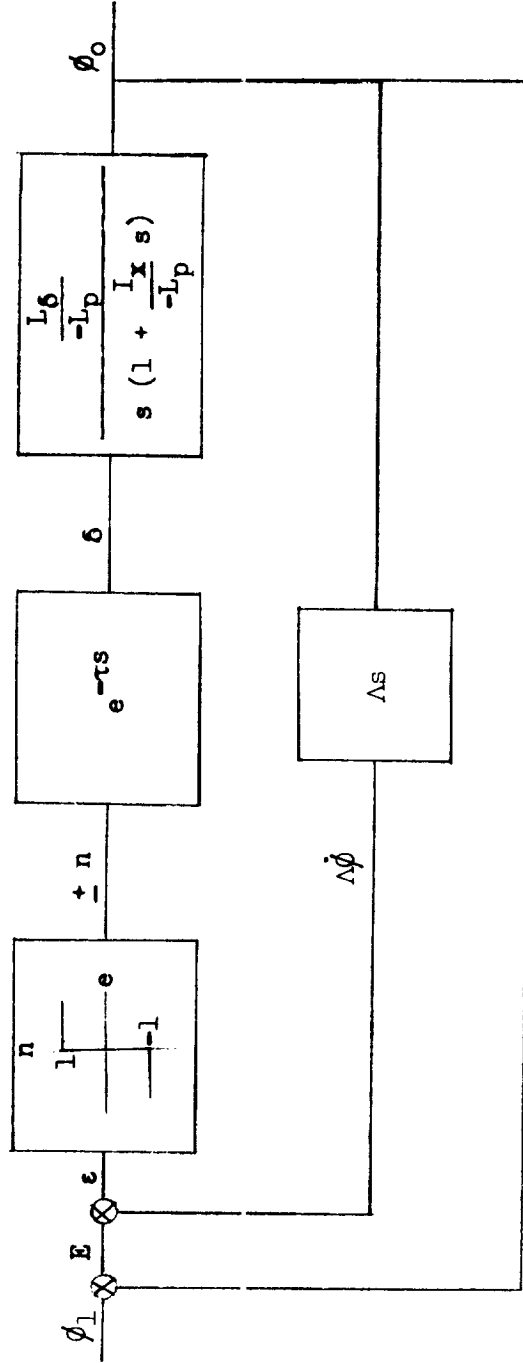


Figure 13.- Concluded.



(a) Designations.



(b) Transfer functions.

Figure 14.- Block diagram of flicker displacement-plus-rate control.